Which processes structure global pelagic ecosystems and control their trophic functioning? Insights from the mechanistic model APECOSM

Laureline Dalaut [a],[*], Nicolas Barrier [a], Matthieu Lengaigne [a], Jonathan Rault [b], Alejandro Ariza [c], Mokrane Belharet [a], Adrien Brunel [a], Ralf Schwamborn [d], Mariana Travassos-Tolotti [a], Olivier Maury [a]

[a] MARBEC, Univ. Montpellier, CNRS, Ifremer, IRD, Sète, France
[b] Ifremer, Plouzané, France
[c] DECOD, Ifremer, INRAE, Institut Agro, Nantes, France
[d] Federal University of Pernambuco, Recife, Brazil

ARTICLE INFO

ABSTRACT

Pelagic ecosystems are distributed throughout the world's seas and oceans. They are characterised by strong vertical structuring, horizontal heterogeneity and temporal variability, which pose significant challenges for modelling them on a global scale. In this paper, we use the mechanistic high trophic level model APECOSM (Apex Predators ECOSystem Model) to assess how the physical and biogeochemical environment constrains the structure and trophic functioning of pelagic ecosystems worldwide.

To this end, we configure the model to represent the three-dimensional and size-structured dynamics of six generic pelagic communities: small and medium epipelagics, tropical tunas, mesopelagic feeding tunas, small coastal pelagics, mesopelagic residents and mesopelagic migrants. We analyse their emergent three-dimensional spatial structuring on a global scale.

We first show that the modelled horizontal and vertical distributions are consistent with the observed data. We then analyse the role of key environmental drivers, such as temperature, light, primary production, currents and oxygen on the response of the communities. Finally, we explore the trophic functioning of pelagic ecosystems, focusing on the emergent diets of communities and their variation with organism size.

This study demonstrates the ability of a mechanistic ecosystem model to represent the multidimensional structural heterogeneity of marine ecosystems globally (encompassing three-dimensional distribution, size variations, and community composition) from a small set of universal principles and well-defined hypotheses. This approach helps to understand how the various processes at stake act and interact to shape the structure of global pelagic ecosystems, and eventually elucidate the heterogeneity of their trophic functioning.

1. Introduction

Marine ecosystems are among the most important reservoirs of the world's biodiversity, with hundreds of thousands of known species (Mora et al., 2011; IPBES, 2019) and many more yet to be discovered — between one third and two thirds of marine species may remain undescribed (Appeltans et al., 2012). Within marine ecosystems, pelagic ecosystems occupy the entire water column but do not interact directly with the benthic ecosystems that occupy the seafloor. Pelagic ecosystems cover most of the world's ocean surface and are home to many species, including iconic large predators such as tunas, billfishes and sharks. They provide essential ecosystem services, such as supporting inshore fisheries for small pelagic fish or offshore

fisheries for large predators. They also play a fundamental role in climate regulation, particularly in sequestering and exporting carbon to the deep sea and seafloor (Robinson et al., 2010; Sanders et al., 2016). Pelagic ecosystems are highly heterogeneous on a global scale. They support very diverse communities whose absolute and relative abundance, sensitivities to environmental drivers, size structure and vertical distribution vary geographically and temporally, at different scales. This structural heterogeneity, in turn, modulates the functioning of pelagic ecosystems and the services they provide to human societies.

However, climate change is driving rapid and dramatic transformations in pelagic ecosystems (IPCC, 2023a; IPCC, 2023b). Physical and biogeochemical changes, such as rising water temperatures, ocean

---

acidification, decreasing oxygen concentrations and primary production, are well underway and are expected to continue and possibly accelerate in the future (e.g. Bopp et al., 2013; Kwiatkowski et al., 2020). These changes are already impacting the biomass of marine animals and their effects are likely to intensify (Lotze et al., 2019; Tittensor et al., 2021), potentially altering the structure and functioning of pelagic ecosystems and threatening the services they provide to humans. In this period of rapid change, understanding the mechanisms that underpin the structural heterogeneity of pelagic systems and control their functioning is key to anticipating their future state and developing robust scenarios of the ocean for the coming decades.

Marine ecosystem models are important tools in this perspective. Beyond enhancing our understanding of the processes involved and how they interact to shape marine ecosystems, they are crucial for projecting ecosystem response to multiple stressors. This is key to understand and anticipate possible futures, develop strategies and implement appropriate management measures to mitigate and adapt to the multiple impacts of climate change.

However, due to the complexity of marine ecosystems and existing knowledge gaps, the projection of marine ecosystem response to climate change is riddled with uncertainty (Tittensor et al., 2021). This uncertainty is exacerbated by the fact that present marine ecosystems are already operating in unprecedented conditions with no historical analogues (Rose et al., 2020). This situation is expected to worsen when models are employed to explore future ecosystem states in oceanic conditions that extend far beyond the range of both past and present observations.

Building ensemble simulations from multiple ecosystem models, rather than relying on a single model, is a way to estimate this uncertainty. Using such an ensemble approach, model intercomparison projects have provided ensemble simulations of how future ecosystems and fisheries may respond to climate change (Lotze et al., 2019; Tittensor et al., 2021). These simulations project a long-term decline in global marine animal biomass under the SSP5-8.5 scenario, reaching 19% by the end of the 21st century in comparison to the end of the 20th century (Tittensor et al., 2021). However, this decline is unevenly distributed and is expected to be larger in tropical regions and for high trophic levels (HTL) (Lotze et al., 2019). While sensitivity experiments have been conducted to disentangle the effects of temperature and low trophic level changes on the projected decline of total animal biomass (Heneghan et al., 2021), an in-depth analysis of the ecological processes underlying these changes has not been undertaken yet. One of the reasons is that the diversity of ecosystem models used to produce the ensembles requires common metrics, which tend to be highly aggregated such as total consumer biomass (Tittensor et al., 2018). This aggregation limits an in-depth analysis of the processes underpinning the effects of climate on ecosystem structure and functioning, which ultimately drive the total biomass decline. With this in mind, the present study aims to analyse, using the detailed mechanistic ecosystem model APECOSM (Apex Predators ECOSystem Model), how the structural heterogeneity of pelagic ecosystems emerges from the heterogeneity of climatic variables (e.g. physical and biogeochemical) and how this affects their functioning in the contemporary ocean.

APECOSM (e.g. Maury, 2010; Maury and Poggiale, 2013) is a 3D, trait-based and size-structured mechanistic model that explicitly represents the processes responsible for the structure and dynamics of marine ecosystems. The principle of APECOSM is to model basic biological and ecological processes at the individual level from a few sets of first principles and simple assumptions, and to allow macroscopic ecosystem structure and function to emerge from the interactions between individual dynamics and the physical–biogeochemical environment. This generic and adaptive approach enables the identification and weighting of the role of the different processes shaping the ecosystem structure and dynamics in various environments, from local to global scales. APECOSM can be configured to represent the dynamics and interactions of a predefined set of functional communities. These are essentially characterised by the size of the species constituting the community, their diurnal or nocturnal behaviour, the size range of prey available to predators, and their physiological sensitivity to temperature, oxygen and light. The model was initially configured to represent 3 generic communities: the epipelagic, the mesopelagic migrant and the mesopelagic resident communities (Maury, 2010). This archetypal configuration has been applied in various contexts : for instance to contribute to global climate change projections (e.g. Novaglio et al., 2024, Lefort et al., 2015), to study the mechanisms underpinning ecosystem response to ENSO in the Pacific (Barrier et al., 2023) or to assess the effects of iron fertilisation on marine ecosystems (Tagliabue et al., 2023).

In the present paper, we introduce a new configuration of APECOSM that considers six communities, enabling a more detailed analysis of pelagic organisms ecology. This updated configuration is also in line with the need to assess exploited large pelagic, small pelagic and benthic-demersal organisms (the latter is not currently represented in APECOSM) in future marine ecosystem model intercomparison exercises (Blanchard et al., 2024, Maury et al., 2025) . In our configuration, the epipelagic community is subdivided into four communities to distinguish small offshore forage organisms from cold-water coastal pelagics (e.g. sardines-anchovies) and from large oceanic top predators, which are in turn subdivided into surface-feeding and deep-feeding organisms.

The main objective of this paper is to use the APECOSM model to analyse how pelagic ecosystems are structured by the heterogeneity of the physical and bio-geochemical environment on a global scale, and how this affects their trophic functioning. To do this, we first evaluate our new six-communities configuration over the historical period by comparing it to existing data. Using a combination of scientific literature, acoustic observations, empirical models derived from a global acoustic dataset, satellite-measured fishing effort distribution, fishing data, and basin-scale measurements of the biomass size-spectrum from plankton to fish, we show that APECOSM succeeds in bringing out the multidimensional (i.e. horizontal, vertical and size-structural) heterogeneity of marine ecosystems, as reflected in the diverse datasets used. We examine the results on a global scale to describe the ecological phenomena at play and illustrate the distinctive characteristics of the communities represented. We identify the processes involved and how they interact to produce structural patterns that resemble observations. The regional and seasonal variations of this global-scale picture are explored in Dalaut et al. (in prep.) by comparing some contrasting regions to the global mean state.

Finally, after exploring how the environment structures pelagic ecosystems, we show how the model contributes to our understanding of their trophic functioning. To this end, we elucidate the vertical and horizontal distributions of the different communities and delineate how they give rise to specific trophic interactions between them. This offers insights into predation mechanisms and interactions among communities.

The paper is organised as follows: Section 2, introduces the physical and biogeochemical models driving APECOSM (Section 2.1), provides an overview of APECOSM's functioning (Section 2.2.1), and details the configuration of the modelled communities (Section 2.2.2), as well as the simulation setup (Section 2.3). Section 2.4 presents the observational data used for model assessment. In Section 3.1, we evaluate the ecosystem structure emerging from the model by comparing it with observational data. Section 3.2 explores how ecological interactions emerge from the structure, providing insights into their trophic functioning. Finally, Section 4 provides a brief summary and a discussion on the contribution of these results to our understanding of pelagic ecosystems.
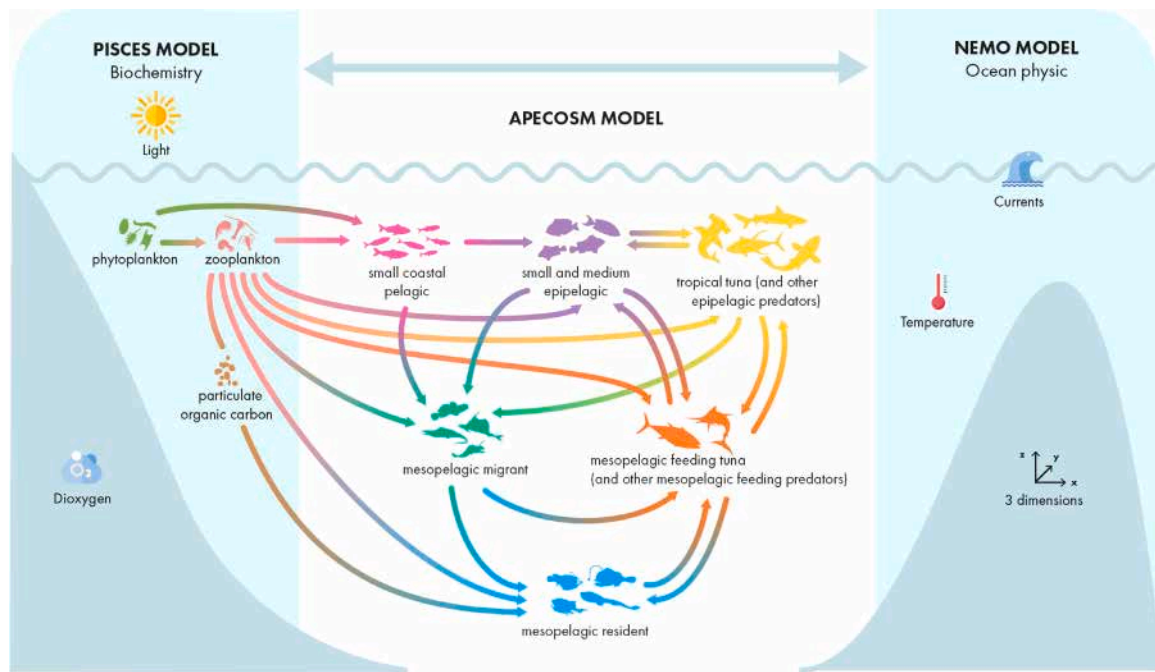
Fig. 1. Schematic of the APECOSM configuration featuring 6 generic high trophic level communities. The high trophic level model APECOSM uses physical and biogeochemical forcing from the NEMO and PISCES models. The arrows indicate the direction of potential trophic interactions.

2. Methods and tools

APECOSM (Apex Predators ECOSystem Model) is the marine ecosystem model used in this study. This model employs a mechanistic approach based on first principles and a few sets of elementary assumptions formulated at the individual level to describe the dynamics of high trophic levels (HTLs) (e.g. Maury, 2010). APECOSM is driven by the three-dimensional physical and biochemical fields simulated by the physical ocean model NEMO-v3 (Madec, 2015) coupled to the biogeochemical model PISCES-v2 (Aumont et al., 2015). The three-dimensional forcing variables used to force APECOSM include temperature, currents, oxygen, light and concentrations of low trophic level (LTL) groups : flagellates and diatoms, micro- and meso-zooplankton, small and large particulate carbon (Fig. 1). The NEMO-PISCES coupled model is briefly described in Section 2.1, while APECOSM is presented in Sections 2.2.1 and 2.2.2.

2.1. The physical and bio-geochemical models

The dynamic state of the ocean is simulated using the NEMO-v3.6 modelling platform (Madec, 2015). The ORCA1 global numerical grid used here to integrate the model has a nominal horizontal resolution of 1°, refined to 1/3°meridionally in the equatorial band. The ocean model features 75 vertical levels, with a vertical resolution ranging from 1 m at the surface to 100 m at 1 km depth, which varies over time following Bruno et al. (2007). Topography is represented using partial-step thicknesses (Barnier et al., 2006). The model outputs, such as temperature and currents, serve as inputs for the biogeochemical model PISCES.

The marine biogeochemical model PISCES-v2 (Aumont et al., 2015) simulates the sources and sinks of 24 prognostic variables. The model represents LTLs using two phytoplankton groups (nanophytoplankton and diatoms) and two zooplankton size classes (microzooplankton and mesozooplankton). Phytoplankton growth is regulated by five limiting nutrients (Fe, PO4, Si(OH)4, NO3, and NH4) in addition to light and temperature. PISCES-v2 includes three nonliving compartments: semi-labile dissolved organic matter and two size classes of particulate

organic matter (POM), which differ in size (1–100 μm for small particles and 100–5000 μm for large particles) and sinking speed.

LTL and POM groups from PISCES serve as potential food sources for the HTL organisms simulated by APECOSM. To be compatible with the size-structured predation of APECOSM, we assume that their log–log size distributions are linear with an arbitrary slope fixed at −1 over their respective size ranges. Neither PISCES nor the configuration of APECOSM used here explicitly simulates macrozooplankton (i.e. planktonic organisms ranging in size from a few millimetres to a few centimetres). In order to avoid a discontinuity between the two models and to bridge the gap between the PISCES planktonic organisms and the APECOSM HTL communities, a macrozooplankton community proportional to the PISCES mesozooplankton is included among APECOSM forcings, assuming that it consists of individuals between 2 mm and 5 cm in size, distributed according to a linear log–log size-spectrum aligned with the PISCES mesozooplankton (See Appendix A).

2.2. Marine ecosystem model

2.2.1. APECOSM generalities

The NEMO and PISCES models feed into APECOSM (Maury, 2010) to produce emergent dynamics of HTL communities. APECOSM is an Eulerian ecosystem model that provides a mechanistic derivation of the three-dimensional dynamics of size-structured pelagic communities by integrating individual and population level processes. At the individual level, it models individual energy uptake, utilisation, growth, development, reproduction, somatic and maturation maintenance according to the Dynamic Energy Budget (DEB) theory (Kooijman, 2010).

The DEB theory is a comprehensive mechanistic theory of metabolism that has undergone extensive empirical testing. In the framework of the DEB theory, food, temperature, as well as body size affect individual metabolism including growth and reproduction. Because fish are ectothermic, their body temperature varies with the environment, although they can partly control it by behavioural adaptation (changing depth according to water temperature or increasing/decreasing muscle work). Within community-specific temperature ranges, the higher the internal temperature, the higher the metabolic
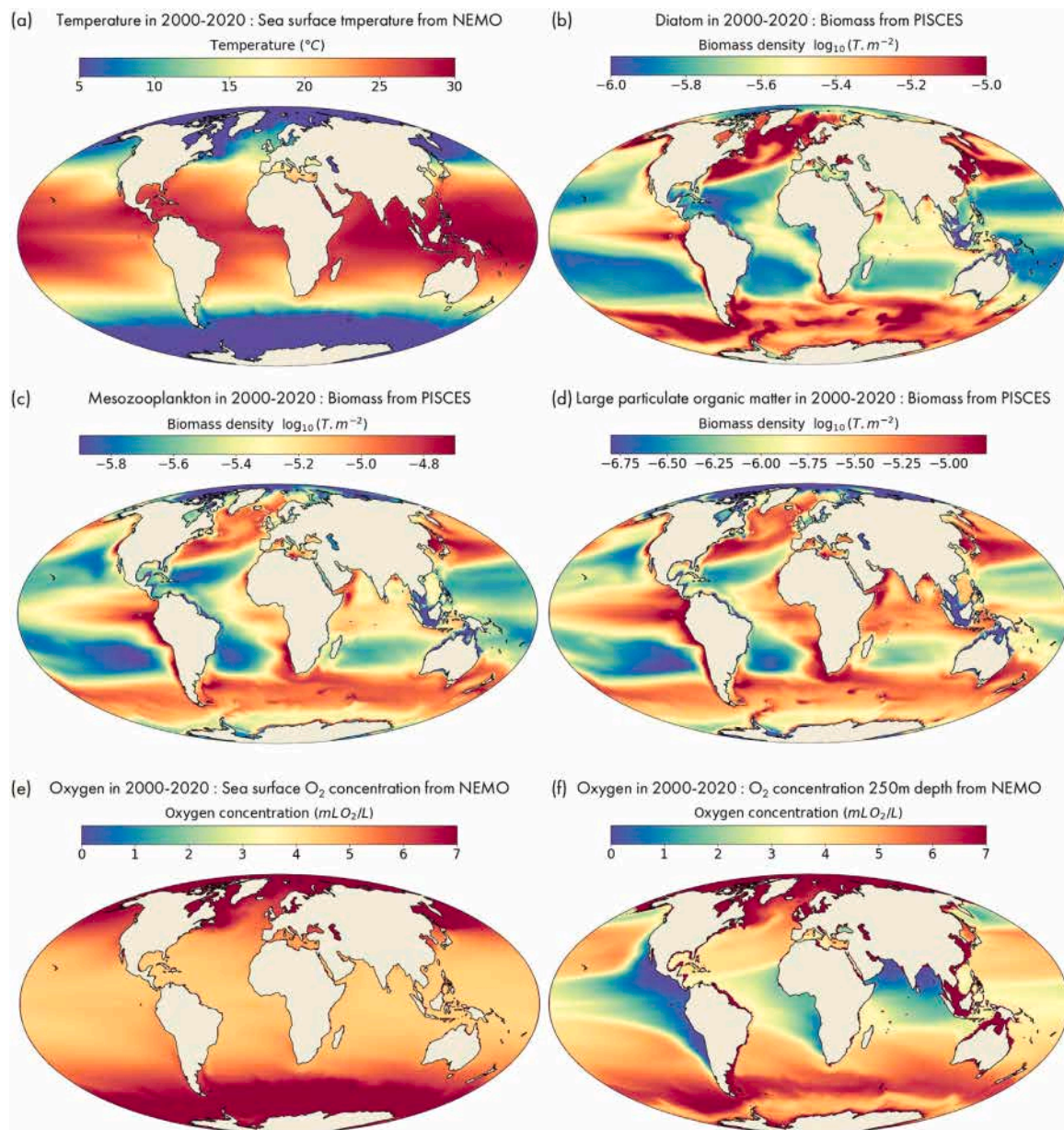
Fig. 2. NEMO-PISCES forcings. Sea surface temperature from NEMO (a). Low trophic level horizontal distribution from PISCES : Large phytoplankton (diatoms) (b), mesozooplankton (c), large particulate organic mater (d). Oxygen concentration at the surface (e) and at 250 m depth (f) where OMZ are visible is blue.

rate, as temperature accelerates the biochemical processes at the base of metabolism. This means that an ectotherm with a higher internal temperature can swim faster to hunt or escape from a predator, but needs more energy to meet somatic maintenance needs. This relationship between metabolism and temperature is well described by a mixture of Arrhenius relationships (e.g. Kooijman, 2010, cf. Fig. 3).

In addition to individual metabolism, APECOSM takes into account key physiological aspects like vision and respiration, along with essential processes such as passive transport by marine currents, active habitat-based movements (Faugeras and Maury, 2005) and schooling, which controls predation (Maury, 2017). It also considers ecological processes such as opportunistic size-structured trophic interactions, competition for food, as well as predatory, disease, ageing and starvation mortality. The size-based opportunistic predation assumed in APECOSM means that organism diets reflect local prey availability and predator–prey size ratios, which emerge from the need for predatory fish to have jaws wide enough to swallow their prey. In APECOSM as

in reality, trophic interactions are inherently dynamic; every organism has the potential to be both predator and prey, depending on its relative size (Maury, 2010).

Finally, to consistently integrate individual dynamics to population and to community levels, and to account for life-history diversity within communities, APECOSM uses a trait-based approach (Maury and Poggiale, 2013, cf. Fig. 4). In a nutshell, each community is assumed to comprise a large number of species within a given range of maximum species size. Since the individual size-dependent metabolism of a given species depends on its asymptotic size in the DEB theory (Kooijman, 2010; Maury et al., 2018), the resulting metabolism at the community level depends on the relative abundance of each species in the community, from the smallest to the largest. As this relative abundance of species within a community varies dynamically and regionally in APECOSM, so do the rates controlling energetics and trophic interactions at the community level.
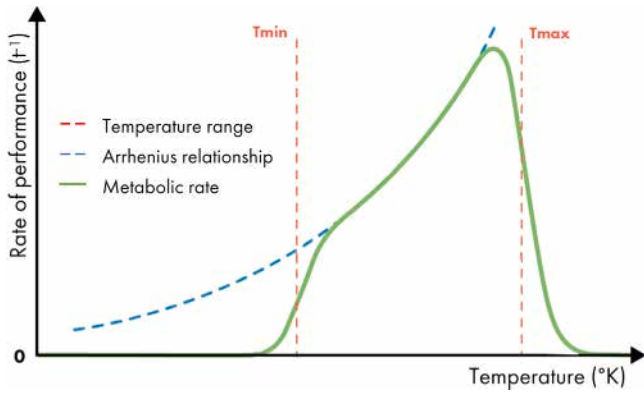
Fig. 3. APECOSM uses the Dynamic Energy Budget (DEB) theory where temperature affects metabolism, including growth and reproduction, according to an Arrhenius relationship (blue dotted line). Each community is also characterised by a given temperature range (red dotted lines) and the combination of the two gives the temperature effect on metabolism (green line), which modulates metabolic rates and swimming speed as temperature changes.
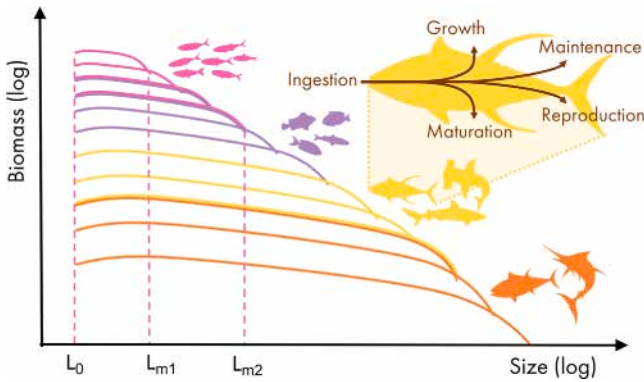

Fig. 4. APECOSM uses an individual-based and a size- and trait-based approach to account for species life-history diversity within communities. The species-level size spectra are derived from the DEB energy fluxes at the individual level, represented by arrows in the zoomed fish. Each community is assumed to encompass a large number of species within a given range of maximum species size characterised by a minimum asymptotic length L_{m1} and a maximum asymptotic length L_{m2}. The minimum size L_0 is assumed to be the same for all species. Since the species distribution within each community varies spatially and temporally, so do the parameters controlling energetics, mortality and trophic interactions at the community level.

The dynamics of communities in the model is determined by integrating the core state equation below:

$$\partial_t \epsilon = \underbrace{-\partial_w(\gamma\epsilon) + \frac{\gamma}{w}\epsilon}_{\text{growth}} - \underbrace{M\epsilon}_{\text{mortality}} - \underbrace{\vec{\nabla}\cdot(V\epsilon)}_{\text{advection (3D)}} + \underbrace{\vec{\nabla}\cdot(D\vec{\nabla}\epsilon)}_{\text{diffusion (3D)}}$$

Where ϵ represents the biomass density of organisms in the community, w denotes their individual weight, γ is the growth rate, M encompasses various mortality rates, calculated using equation 12 from Maury and Poggiale (2013), V and D are the sum of 3D passive and active velocities and diffusivity coefficients computed following Faugeras and Maury (2005). The growth contribution is made of an advection (i.e. the biomass transfer along the size-spectrum, left-hand side) and a source term (i.e. increase of biomass due to individual growth, right-hand side) (Maury and Poggiale, 2013).

2.2.2. APECOSM: configuration

APECOSM enables the simulation of distinct interactive generic communities sharing the same rules of functioning, but distinguished by a small set of parameters that are detailed below and summarised in Fig. 5. In the present model configuration, we simulate 6 communities:

1. Small and medium-sized epipelagic
2. Tropical tuna
3. Mesopelagic migrant
4. Mesopelagic resident
5. Mesopelagic feeding tuna
6. Small coastal pelagic

These communities were selected based on their ecological importance in marine pelagic ecosystems. Collectively, they cover the majority of pelagic species from the surface to 1000 m depth. The commercial value of tuna, small coastal pelagic fish and some species of the small and medium-sized epipelagic community is considerable, making them vital resources to the livelihoods of human populations reliant on fishing. Mesopelagic organisms constitute a substantial biomass, largely exceeding that of the epipelagic biomass (Irigoien et al., 2014; Proud et al., 2019). While being largely unexploited, these species face potential threats from industrial exploitation plans (Grimaldo et al., 2020; Olsen et al., 2020). Bathypelagic and abyssopelagic species, which inhabit the deepest parts of the ocean, are not considered in this study as they remain understudied, which would make their modelling both challenging and highly speculative. In this section, we detail the configuration of each community in terms of temperature range, light sensitivity, range of maximum species length, predator/prey size ratios and their diurnal or nocturnal behaviour, as established in existing literature.

The small and medium epipelagic community

The small and medium epipelagic community is a very generic community, representing a wide range of species inhabiting in the open ocean. This community encompasses all species that are not represented by the other epipelagic communities (i.e. the small coastal pelagics and tunas). These organisms are functionally important in the model, ensuring a trophic continuity as they forage on plankton and small fish and in turn serve as prey for large predatory fish. Some of the species in this community also hold commercial value, such as sardinellas (*Sardinella spp.*), Chilean jack mackerel (*Trachurus murphyi*), chub mackerel (*Scomber japonicus*) or pandora (*Pagellus erythrinus*).

The species included in this community are numerous but often poorly studied, with the exception of those that are commercially exploited (Kizenga et al., 2021; Lteif et al., 2020). They typically reside above the thermocline, spending the majority of their life cycles within the upper 20 to 30 metres (Collette, 2010).

In this community, we decided to include species with a maximum size ranging from 11 to 84 cm to distinguish them from the two top predator communities on the one hand, and from macrozooplankton on the other. Their vertical distribution is mainly limited by the light range in which they see their prey during the day in shallow waters, the availability of food (e.g. prey biomass concentration and the tendency for prey to form schools at the depth where predators can detect them) and their temperature limits that we have set between 8 and 31 °Celsius to cover the entire latitudinal range of pelagic fish distribution in the global ocean (Galbraith et al., 2019).

The tropical tuna community

This community is designed to include all the epipelagic tropical top predators that forage in shallow open ocean waters during the day. It includes species of major commercial importance like yellowfin tuna (*Thunnus albacares*) or skipjack tuna (*Katsuwonus pelamis*) as well as less intensively exploited species such as sailfishes (*Istiophoridae*), wahoo (*Acanthocybium solandri*) or dolphinfishes (*Coryphaenae*), among others. Functionally, this top predators community stabilises the pelagic food chain by exerting predation on smaller, more variable species (Maury, 2017).

Given the high commercial value of tuna, comprehensive fisheries data as well as many scientific studies are available (e.g. Miyake et al., 2010), providing a comprehensive view of their spatial dynamics, movements, physiology, growth, and feeding habits.

Fig. 5. The APECOSM model uses the same generic mechanistic approach to model the dynamics of each of the 6 high trophic level communities. The communities are only distinguished by a small number of key physiological and behavioural parameters: the range of maximum species size within a community, light sensitivity, diurnal or nocturnal feeding behaviour, predator/prey size selectivity ratios and sea surface temperature limits. Epipelagic fishes can only see in the high light intensities that occur at the ocean surface during the day, while mesopelagic communities are adapted to see in dark waters. We assume that all communities feed during the day, except for mesopelagic migrants, which feed at night. Predation is controlled by the size of the predator relative to its prey, which is the same for all communities except for small coastal pelagic fish, which feed on organisms much smaller than themselves. Temperature preferences also play a key role in determining the spatial and vertical distribution of communities, with the exception of mesopelagic migrants and residents, which have no temperature range. Equations and their parameters are detailed in Supplementary (Appendix B and C).

In our model configuration, we limit the tropical tunas community to warm waters from 18 to 31 °Celsius (Fujioka et al., 2024; Andrade, 2003; Lu et al., 2001). This temperature range, combined with the distribution of available food, advection by ocean currents and active movement towards favourable areas, determines their global distribution. We set the maximum species size range of this community to be between 84 and 196 cm to include the key species listed above.

The mesopelagic migrant community

Mesopelagic fishes, both migratory and non migratory, are considered the most abundant vertebrates on Earth, inhabiting vast areas of the ocean from the surface to about 1000 m depth (St. John et al., 2016; Irigoien et al., 2014; Proud et al., 2019). The mesopelagic migrants, such as lanternfishes (*Myctophidae*, *Notoscopelidae*), lightfishes (*Phosichthyidae*), or hatchetfishes (*Sternoptychidae*), participate in the largest migration happening on Earth : every evening, as the sunlight fades, billions of animals migrate up into the epipelagic zone to forage, returning to deeper mesopelagic waters in the morning. Other non-fish organisms, such as flying squids (*Ommastrephes bartramii*), the larger jumbo squids (*Dosidicus gigas*), or large fish predators such as the lancet fish (*Alepisaurus ferox*) are also part of the mesopelagic migrant community.

Mesopelagic migrants data mainly come from direct observational studies (e.g. Caiger et al., 2021; Eduardo et al., 2024; Drazen and Sutton, 2017) or acoustic surveys (e.g. Ariza et al., 2022). However, compared to epipelagic and coastal fish species, very little is known about their life history (Martin et al., 2020), feeding habits and behaviour, due to their inaccessibility and historical lack of commercial interest.

To take into account the ecological characteristics of migratory mesopelagic species, which are nocturnal and feed in surface waters, their light sensitivity was set to match the average light intensity found at night in the upper tropical and subtropical ocean. Their sensitivity to oxygen was set to capture their avoidance of oxygen minimum zones (OMZ). We considered that the maximum species size within this community ranges from 8 to 196 cm for the largest species.

The mesopelagic resident community

Unlike migratory mesopelagics, the resident mesopelagic community encompasses organisms that reside permanently at depths between 200 m and 1000 m. The mesopelagic resident community includes a wide variety of fish and cephalopod species with very different sizes and life histories (e.g. Eduardo et al., 2024), such as the ubiquitous genus *Cyclothone*, *Stomiidae*, *Alepocephalidae* or *Ceratioidea* (Eduardo et al., 2024; Sutton, 2013; Priede, 2017). The bulk of this community biomass is dominated by a few small species, in particular Cyclothones (*Cyclothone spp.*), which are often claimed to be the most abundant of all vertebrates on earth and measure between 1.6 cm to 5.3 cm (Thompson and Kenchington, 2017; Granata et al., 2023).

These organisms are often ambush feeders that largely rely on bioluminescence to attract their prey in the dark, deep waters of the mesopelagic zone (Young, 1983; Herring, 1977). They are assumed to be diurnal in the model, to be able to feed on migratory species that descend to these depths during the day. To use bioluminescence efficiently for predation, these species require the dark conditions that are found in deep mesopelagic waters during daytime. Their light sensitivity in the model therefore reflects the dark conditions that prevail in mesopelagic waters during the day. Like mesopelagic migrants, they can be exposed to low oxygen concentrations and their response to oxygen levels is modelled similarly. In the model, the species maximum size range is assumed to be the same as for the mesopelagic migrant community, ranging from 8 to 196 cm.

The mesopelagic feeding tuna community

The mesopelagic feeding tuna community typically represents the ecological specificity's of bigeye tuna (*Thunnus obesus*). It also includes other epipelagic top predators that are feeding on deep mesopelagic organisms during the day such as swordfish (*Xiphias gladius*). Juvenile bigeye tuna, up to about 80 cm, schools with skipjack and yellowfin tuna and hunt in surface waters (Romero et al., 2021) where they are caught by the purse seine fisheries targeting these species. As they grow, they acquire thermoregulatory abilities that allow them to exploit the abundant mesopelagic resources that live at depth in colder waters

(e.g. Graham and Dickson, 2004). Their diving depth increases with body size (Hino et al., 2019; Maury, 2005). Swordfish do not have such efficient thermoregulatory capabilities, but their large mass gives them enough thermal inertia to stay in cold waters for long periods of time.

These fishes have been extensively studied, with a focus on their fisheries and their thermoregulatory capacity (Hino et al., 2019; Brill et al., 2005; Thums et al., 2013). During the night, they stay mostly near the surface, where temperatures are warmer. At dawn, they descend below the thermocline to track prey organisms of the vertically migrating deep-scattering layer down to the mesopelagic zone (Fuller et al., 2015).

In the model, we hypothesise that the physiological responses of juveniles in this community to temperature, light and oxygen would be similar to those of the tropical tuna community. Their behaviour shifts at around 80 cm in length, giving them greater thermal tolerance and changing their sensitivity to light so that they can feed at depth. The maximum species size for this community is set between 2 m and 2.5 m.

The small coastal pelagic community

Small coastal pelagic fishes, such as anchovies (*Engraulidae*), sardines (*Sardina pilchardus*, *Sardinops sagax*) and sprats (*Sprattus spp.*), are among the most commercially exploited fish species in the world, contributing significantly to global fisheries catches. These organisms inhabit productive ocean regions, particularly the Easter Boundary Upwelling Systems (EBUS ; including the Benguela, California, Canary and Humboldt upwellings). They are mainly used for producing fishmeal and fish oil for the aquaculture industry but are also part of the diet of many coastal populations.

Due to their commercial importance, substantial fisheries data and literature reviews have been produced on these species (e.g. Espinoza et al., 2009; Checkley et al., 2017; Hernández-Santoro et al., 2019; Izquierdo-Peña et al., 2019). These small plankton feeders are the main forage source for larger fish, but also for marine mammals and seabirds in upwelling regions.

In our model, we increased the minimum and maximum predator–prey size ratio of the small coastal pelagics community so that it can feed on plankton throughout its size range. We restricted the community temperature limits to relatively cold waters (between 12 °Celsius and 21 °Celsius) to limit its distribution to the upwelling and temperate waters. Additionally, their mortality is adjusted to reflect the high predation on their schools by warm-blooded animals, which are not explicitly represented in APECOSM. Being small forage fish, the maximum size of the species included in this community ranges from 13 to 41 cm.

Our model is implemented on the ORCA1 numerical grid (also used by the NEMO-PISCES models), whose spatial resolution of 1° is too coarse to capture the complex meso- and submeso-scale processes controlling the dynamics and spatial distribution of small coastal pelagic fishes populations (Ragoasha et al., 2019; Lett et al., 2015; Mullon et al., 2003; Bakun, 1998; Alcaraz, 1997; Cury and Roy, 1989). In particular, the retention of eggs and larvae of small pelagic fishes in upwelling cells, which is one of the three pillars of the ecology of these species identified in the Bakun Ocean triad (enrichment, concentration, retention, e.g Bakun, 1998), is not captured at this coarse resolution. To mitigate this limitation and maintain the community in the upwelling regions, we deactivated the effects of passive transport by ocean currents, preventing this community from dispersing far from the regions where it occurs in reality.

2.3. Simulation setup

To initialise the model, we first conducted a long spin-up simulation forced one-way with linearly detrended atmospheric inputs derived from the JRA-55 atmospheric reanalysis (Kobayashi et al., 2015) over the 1958–2022 period. This strategy effectively removes long-term climate change signals from the forcing, while preserving interannual

to multidecadal signals (for further details on the detrending methodology, see Lengaigne et al., 2024). This spin-up is cycled five times, resulting in a 325-years spin-up simulation. The final timestep of this spin-up serves as the initial conditions for a simulation starting in 1958 and forced with original JRA-55 atmospheric inputs over the 1958–2022 period. This simulation has previously been used to drive APECOSM in Barrier et al. (2023) to explore the epipelagic ecosystem response to ENSO.

After a 65-year spin-up run forced with the NEMO-PISCES spin-up simulation based on the detrended JRA forcing outputs to ensure that each community reaches a stationary state, APECOSM is then forced one-way with the output of the NEMO-PISCES simulation. This simulation is forced with the original JRA-55 atmospheric fluxes over the period 1958–2022, which include both realistic variability and the climate change signal. This 65-year APECOSM simulation is the subject of our analysis in this article.

2.4. Observational data used

To assess the robustness of the model, we compare our APECOSM simulation with observations. We also verify that the modelled size-spectrum slope conforms with theory (e.g. Guiet et al., 2016). In this section, we describe the different datasets used.

2.4.1. Empirical model based on sonar observations

To evaluate the reliability of the model, we compare the horizontal distribution of the total biomass predicted by APECOSM, as well as the mesopelagic migrant and resident biomass, with estimates from a statistical model of sonar-based water-column acoustic backscatter measurements based on environmental predictors (Ariza et al., 2022), which serve as an empirical proxy for pelagic biomass.

This comparison excludes subpolar and polar regions because the backscatter drops dramatically beyond 40 degrees latitude due to changes in the acoustic properties of pelagic fauna (Ariza et al., 2022; Dornan et al., 2019; Chapman et al., 1974). As a result, the acoustic density gradient between temperate and polar latitudes (beyond 40 degrees latitude) do not represent a realistic biomass gradient and must therefore be excluded.

To determine the spatial distribution of the mesopelagic migrant organisms from the empirical model, we computed the cell by cell difference between the 2000–2020 annual average of the acoustic backscatter signal at depths above 200 m at night and during the day. This approach isolates the migratory signal associated with organisms moving into shallower waters at night. For the mesopelagic resident community, we used the acoustic signal detected at depths below 200 m at night, capturing organisms that remain at depth without vertical migration.

The acoustic model used does neither consider depths above 20 m, where a large fraction of epipelagic organisms live, nor does it incorporate the advection effects by marine current that are major drivers of the horizontal distribution of epipelagic fish (Watson et al., 2015). Consequently, we considered that a direct comparison of the empirical distribution that could be estimated for epipelagic organisms (acoustic signal above 200 m during the day) with that of the corresponding epipelagic community from APECOSM would be inaccurate and instead used fishing effort data as a proxy for epipelagic biomass.

2.4.2. Fishing effort based on Automatic Identification System (AIS): Global Fishing Watch data

We used satellite observations of fishing effort as a biomass proxy to assess the global distribution of the epipelagic community simulated by APECOSM. To do this, we used the Global Fishing Watch data from 2012 to 2020 that are publicly available from source data providers : https://globalfishingwatch.org/dataset-and-code-fishing-effort. This dataset covers the fishing activities of more than 70,000 fishing vessels thanks to their Automatic Identification System (AIS) (Kroodsma et al.,

2018). It includes various fishing gears (drifting longlines, purse seines, trawlers, fixed gear, squid jigger and other fishing) and covers different target species mostly fished in epipelagic waters.

2.4.3. Tuna fishing catch data from the SARDARA database

In order to assess the spatial distribution of the tropical tuna and the mesopelagic feeding tuna communities, we used commercial catch data from the SARDARA project, which provides a global scale dataset of geo-referenced catch and effort data for tuna fisheries from 1950 to 2022 (Taconet et al., 2018). This database gathers and standardises publicly accessible tuna fisheries data from four tuna Regional Fisheries Management Organizations (RFMOs): the International Commission for the Conservation of Atlantic Tunas (ICCAT), the Indian Ocean Tuna Commission (IOTC), the Inter-American Tropical Tuna Commission (IATTC) and the Western-Central Pacific Fisheries Commission (WCPFC).

For this analysis, we considered only data with known gears and species. The tropical tuna community, gathering skipjack and yellowfin tuna, is primarily fished by purse seines, generally targeting fish longer than 30 cm, and longlines, targeting fish longer than 1 m. The mesopelagic feeding tuna community is compared with bigeye and swordfish catches, which are mainly caught at greater depths with longlines and at lengths greater than 1 m. In addition to purse seine and longline, the other gears considered in the data for those fish are handlines and hand-operated pole-and-lines, as well as gillnets. A small portion of the catches also come from trawler and small-scale fishing gears such as harpoons, beach seines, and fences.

2.4.4. Qualitative distribution data of small coastal pelagic

No comprehensive dataset was available to assess the modelled spatial distribution of the coastal small pelagic community. In the absence of quantitative data, we used the qualitative map of the spatial distribution of sardines and anchovies from Checkley et al., 2017 (Fig. 7.h).

2.4.5. Acoustic data from the Malaspina expedition

We used acoustic data from the round-the-world Malaspina Expedition (Irigoien et al., 2021; Duarte, 2015; Martinez et al., 2020) to assess the vertical distribution of the biomass simulated by APECOSM in various regions of the global ocean. The expedition operated from December 2010 to July 2011 and collected day and night acoustic data at 122 stations. The 38 kHz echosounder data were compiled at each station from 0 to 1000 m with a 10 m vertical resolution and used as a proxy for the vertical distribution of biomass (Belharet et al., 2024). We selected two types of patterns: the "low oxygen concentration" pattern located in the eastern tropical Pacific OMZ region, with stations where oxygen concentrations are less than 1 mg O2/L between 200 m and 1000 m depth, and the "general pattern" with stations with more than 1 mg O2/L in the water column (Fig. 10.a).

2.4.6. Tuna fishing catch data from the Indian Ocean Tuna Commission (IOTC)

We compared the community size spectrum simulated by APECOSM to IOTC catch and size-frequency data from 2015 to 2020. These data allowed to assess the compatibility of the tuna biomass size distribution simulated in this region with the catches size-frequency. The dataset covers the entire IOTC region, which encompasses the Western and Eastern Indian Ocean. It includes information on various tuna species, such as yellowfin tuna, bigeye tuna, skipjack tuna, bullet tuna, longtail tuna, frigate tuna, as well as other large predators, including narrow-barred Spanish mackerel and kawakawa. The gear considered are mainly purse seine, bait boat, gillnet, line and longline. For the three main tuna species (yellowfin, bigeye and skipjack), raised catch-at-size tables were provided by the IOTC Secretariat. These datasets are produced for stock assessment purposes and represent the best available scientific estimates. For the other species (bullet tuna, longtail tuna, frigate tuna, narrow-barred Spanish mackerel and kawakawa), the size

frequency datasets were used to derive gear selectivity histograms, which were then scaled up to total catches using the nominal retained catches dataset which contains the best scientific estimates for IOTC species. The size frequency and nominal catch datasets are publicly accessible from the IOTC web page: https://iotc.org/data/datasets.

2.4.7. Size-distribution of plankton and mesopelagic fish in the atlantic from the Triatlas project

Biomass size spectra of phytoplankton, zooplankton and mesopelagic nektonic organisms were compiled and standardised in the framework of the EU H2020 TRIATLAS project, from datasets collected independently across the Atlantic Ocean from 1966 to 2023. Different sampling methods were used. For phytoplankton, samples were collected with Niskin bottles between 0 m and 160 m. Zooplankton and mesopelagic organisms were respectively captured between 0 m and 1000 m using multiple opening closing nets (zooplankton) and midwater trawls (mesopelagic fish and invertebrates) (Fock et al., 2024).

3. Global scale analysis and model assessment

3.1. Ecosystem structure

This section evaluates the model ability to simulate the structure of the global pelagic ecosystem using available scientific studies and observational data. To do this, we first compare the horizontal distribution of the six communities that we configured in APECOSM with distribution maps derived from observations (Section 3.1.1). Secondly, we look at the role of the different processes controlling the vertical distribution of the communities in the model, which we compare with acoustic profiles from the Malaspina expedition (Section 3.1.2). Finally, to assess the model behaviour in the size dimension, we examine the emergent biomass size spectra and compare them with available observational data in the Indian and Atlantic oceans(Section 3.1.3).

3.1.1. Spatial distribution : How does the configuration of communities shape their distribution?

The spatial distribution of the individual communities exhibits a great diversity. This diversity arises from their respective configurations (see Section 2.2.2), their interactions with other communities and with the physical–biogeochemical environment. In this section, we compare the average spatial distributions simulated by APECOSM with the various empirical sources described in Section 2.4.

All communities

The horizontal distribution of the different communities in APECOSM is influenced by several factors, including temperature preferences, oxygen sensitivity, spatial distribution of potential prey and their accessibility (vertical distribution, size distribution, visibility and degree of aggregation -schooling-) as well as the effects of advection by marine currents and the size-dependent capacity of organisms to swim actively. The sum of the total biomass of the six simulated communities shows a large-scale spatial pattern similar to the empirical model based on sonar observations (Section 2.4.1), with high biomass in the upwelling regions such as the California Current, Equatorial Pacific, Canary, Equatorial Atlantic and Benguela (Fig. 6.a and Fig. 6.b).

Symmetrically, both models also show a low biomass in the oligotrophic oceanic gyres. Since sonar observations exclude the continental shelf and very shallow waters above 20 m depth (Ariza et al., 2022, cf. Section 2.4.1), the high biomass in the Humboldt Current is likely not well represented in the sonar-based model. In contrast, the APECOSM model captures elevated biomass levels of small coastal pelagic and mesopelagic migrant communities.

Mesopelagic migrant community

Overall, the similarity between APECOSM and the acoustic model is strong. In our APECOSM simulation as in the acoustic empirical model, mesopelagic migrants are very abundant in the Humboldt Current, as
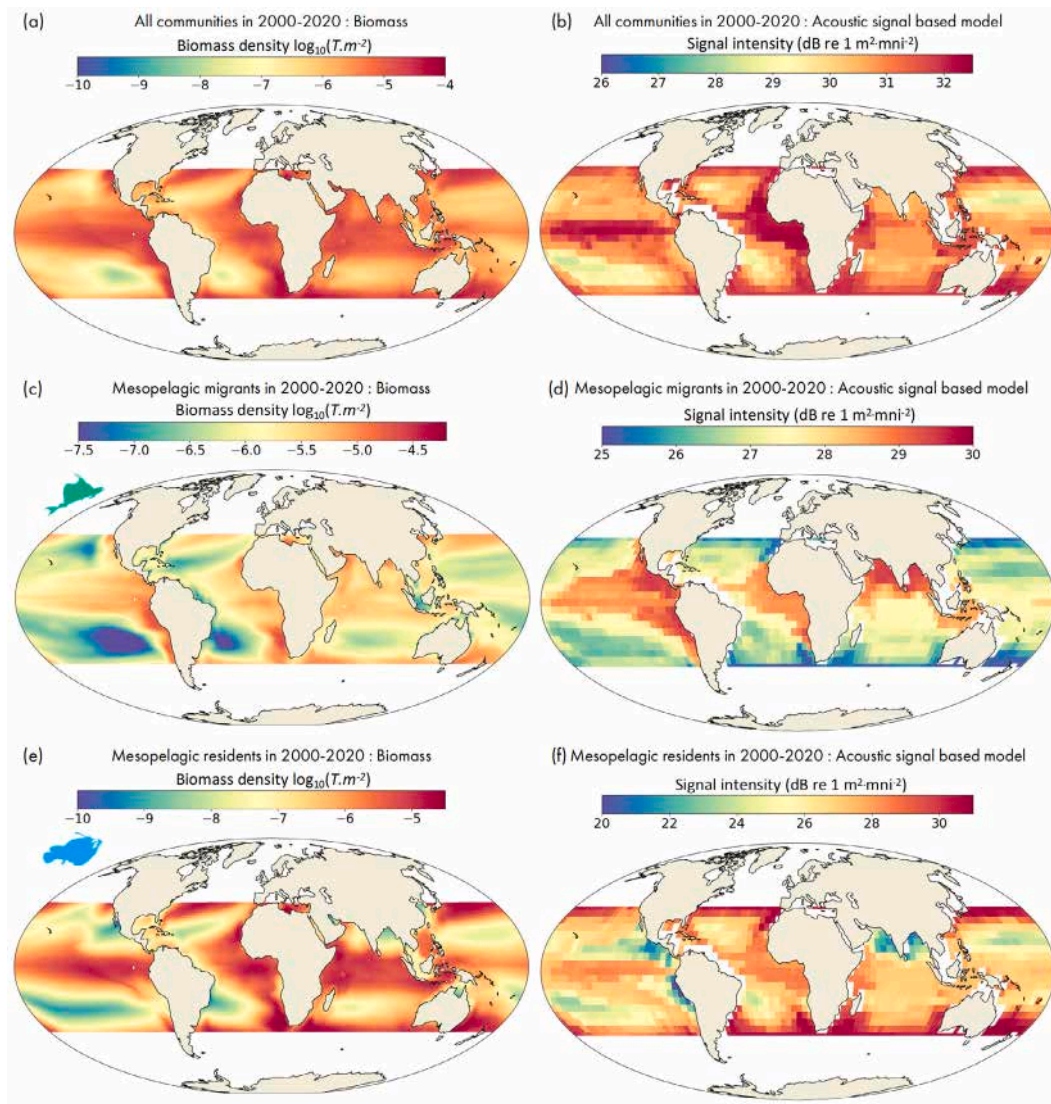
Fig. 6. Average horizontal distributions simulated by APECOSM vs empirical model based on sonar observations. Total depth- and size-integrated annual biomass of all six APECOSM communities (a) and acoustic-based empirical model of the total depth-integrated acoustic signal averaged between 2000 and 2020 (b). The depth- and size-integrated biomass of the mesopelagic migratory community in APECOSM (c) is compared with the empirical model of the acoustic signal in the epipelagic zone integrated from 0 to 200 m depth at night minus the daytime signal integrated over the same depth range (d). The depth- and size-integrated biomass of the mesopelagic resident community in APECOSM (e) is compared to the depth-integrated nocturnal acoustic signal in the mesopelagic zone (depth greater than 200 m) in the acoustic-based model (f).

in other upwelling regions. These regions are favourable areas for their development thanks to their high zooplankton concentrations (Fig. 2.c) in surface waters where this community forages (Fig. 6.c and d). Mesopelagic migrants are also present in OMZs, characterised by low oxygen concentrations between 200 m and 1000 m depth, such as in the eastern tropical Pacific, the Arabian Sea and the Gulf of Bengal (Fig. 2.f). The high abundance of mesopelagic migrants in OMZs, which are also very productive regions (Arabian Sea - Gjosaeter, 1984, Gulf of Guinea - Kobyliansky et al., 2010, Eastern South Pacific Craddock and Mead, 1970), can be attributed to the epipelagic communities confinement to a narrow depth range near the surface (Bertrand et al., 2010), which facilitates predation by mesopelagic migrants at night. In contrast, the rarity of their mesopelagic resident predators in these regions reduces their predation mortality (Fig. 6.e and f).

Mesopelagic resident community

The distribution of the mesopelagic resident community is quite similar in both APECOSM and the empirical model, and is characterised by a worldwide presence, except in the oceanic gyres and OMZs where their abundance is dramatically reduced (Fig. 6.e and f). Mesopelagic

residents normally live in the twilight zone, at depths where oxygen concentrations in the OMZ are very low. In APECOSM, they are therefore confined to shallower waters where oxygen levels are sufficient. However, the higher ambient light levels prevent them from effectively using bioluminescence to attract prey, limiting their ability to maintain high population levels. As a result, they are absent from OMZs such as the eastern tropical Pacific and the northern Indian Ocean (Fig. 2.f), which is consistent with the empirical model.

However, the effect of OMZs on mesopelagic residents appears to be underestimated by APECOSM compared to the empirical model, in particular in the eastern tropical Pacific and the Arabian Sea. This discrepancy could be due to biases in the shape (depth and strength) of the OMZs simulated by PISCES and deserves further investigation. Less conspicuous on the maps, the OMZ off the coast of Angola is also responsible for lower mesopelagic resident biomass in the region in both models (Fig. 6.e and f).

The mesopelagic resident group is the least studied of our six communities, and no field observations are available to confirm the mechanisms that explain their low biomass in the OMZ in APECOSM.
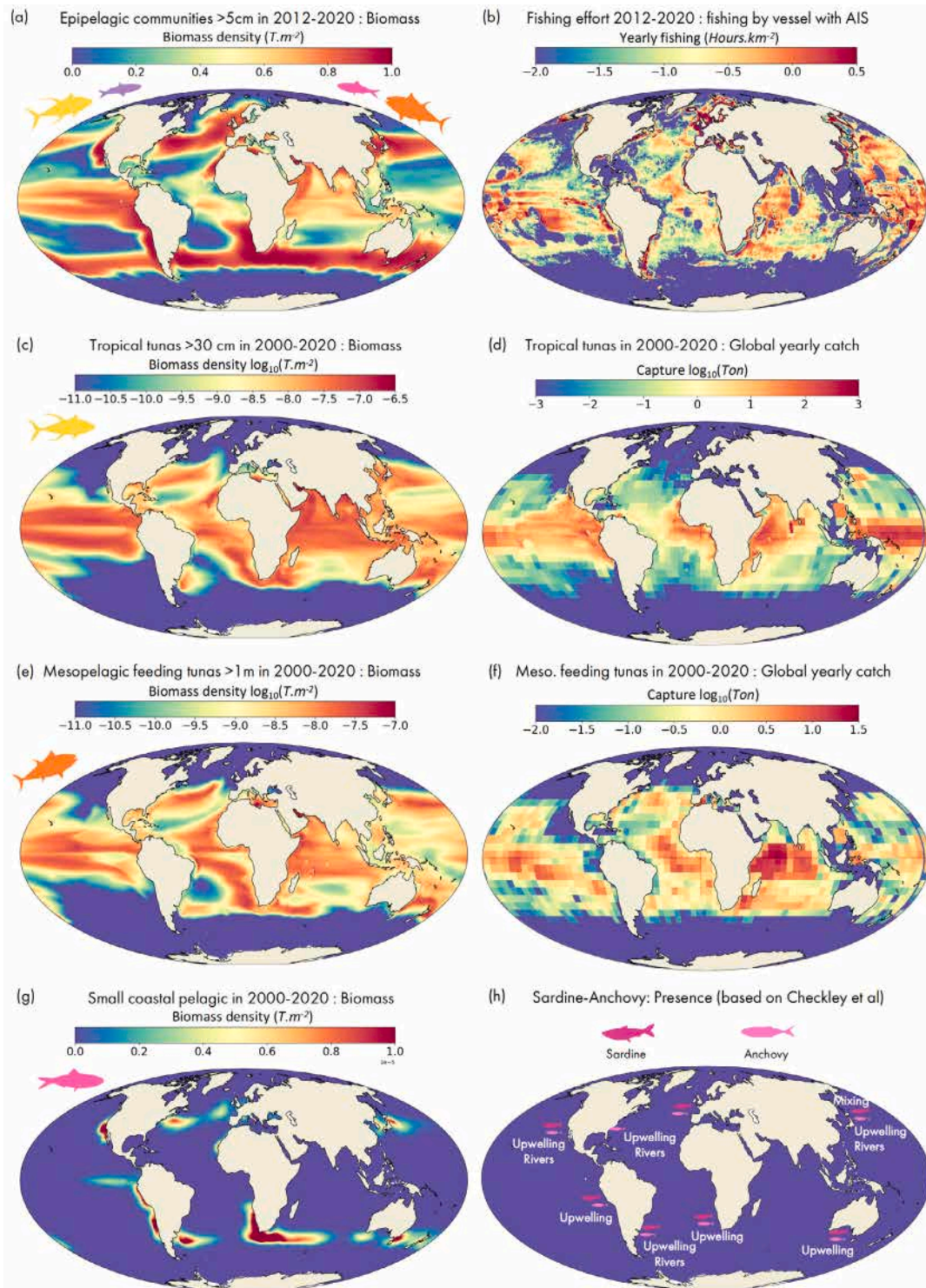
Fig. 7. APECOSM horizontal distributions vs fishing data. The total depth- and size-integrated cumulative biomass of organisms larger than 5 cm of the four epipelagic communities (small coastal pelagic, small and medium epipelagic, tropical tuna and mesopelagic feeding tuna) simulated by APECOSM averaged from 2012 to 2020 (a) is compared with the Global Fishing Watch fishing effort derived from satellite measurements of the AIS signal emitted by fishing vessels during the same period (b). Total depth- and size-integrated cumulative biomass of organisms greater than 30 cm of the tropical tuna community (c) and total skipjack and yellowfin tunas commercial fishery landings averaged between 2000 and 2020 (d). The depth- and size-integrated cumulative biomass of organisms greater than 1 m of the mesopelagic feeding tuna community in APECOSM (e) is compared with the total catch data of bigeyes and swordfish averaged between 2000 and 2020 (f). The depth- and size-integrated biomass of the small coastal pelagic community (g) is compared with a qualitative map of small coastal pelagic population hotspots redrawn from Checkley et al., 2017 (h).

Epipelagic communities

Here we compare the total biomass of organisms larger than 5 cm (fishable size) in the four epipelagic communities that are exploited by commercial fisheries (small and medium epipelagic, small coastal pelagic, tropical tuna and mesopelagic feeding tuna) with the Global Fishing Watch satellite-derived fishing effort, used as a proxy for commercial fish abundance (Section 2.4.2). Overall, there are similarities between the outputs of the APECOSM model (Fig. 7.a) and the fishing

effort based on AIS (Fig. 7.b). At global scale, the epipelagic communities simulated by APECOSM occupy a large area of the globe, except for the southern ocean south to 55°S, and the five nutrient-poor oceanic gyres. AIS-based data agree well with the modelled distribution.

In the five subtropical gyres, the low concentration of primary production is not sufficient to sustain important HTL biomasses and both the simulated biomass and the observed fishing effort are low. However, there is some weak fishing effort in these regions, despite the total epipelagic biomass greater than 5 cm simulated by APECOSM being very low. This fishing effort probably corresponds to fisheries targeting albacore tuna (*Thunnus alalunga*), which is known to inhabit the gyres (e.g. Nikolic et al., 2017). However, the unique ecology of albacore tuna does not align with the communities represented in our model configuration and is therefore excluded from our simulations.

At finer scales, the signature of surface ocean currents that passively transport biomass away from primary production regions is evident in both modelled and observed maps. The effects of the equatorial divergence, which leads to the accumulation of biomass 5°N and S of the equator in the three oceans, are particularly clear, despite the jumbo squid fishery that extends from Peruvian waters to the equator at 115°W, obscuring the observed fishing effort pattern in the Eastern Tropical Pacific (Watch, 2023). The effects of the equatorial current that transports HTL's biomass from the eastern equatorial Pacific waters where primary production takes place to the western equatorial warm pool where it accumulates is also noticeable, as are the effects of the Gulf Stream and the Canary Current in the Atlantic or the Kuroshio current in the Pacific. These patterns demonstrate the importance of biomass redistribution by ocean currents in the epipelagic realm (Watson et al., 2015), which leads to a clear dissimilarity between the spatial distribution of primary production (Huston and Wolverton, 2009, Fig. 2.b) and that of epipelagic fish biomass (Fig. 6.a and b). Nutrient-rich upwelling zones are also clearly visible on both maps, although the low spatial resolution of the model leads to the overestimation of their offshore extent, as in the Humboldt, Canary and Benguela upwellings. The modelled biomass in the Indian Ocean is also very similar to the AIS data, except in the Gulf of Bengal and the Exclusive Economic Zone (EEZ) of Southeast Asian countries, where small-scale fisheries that do not use AIS operate (Taconet et al., 2019).

However, the comparison of the simulated epipelagic biomass with the observed fishing effort reveals discrepancies between about 35°S and 50°S, where APECOSM predicts high epipelagic biomass while fishing effort is relatively low, except for the northern part of this region in the Indian Ocean and southwest Pacific, where the southern bluefin tuna (*Thunnus maccoyii*, SBFT) fisheries operate. SBFTs do indeed forage in the southern oceans, including these regions, and their foraging grounds extend quite far south up to about 50°S (Muhling et al., 2017; Patterson et al., 2018). The small nektonic prey that SBFTs hunt must therefore be very abundant, as simulated in APECOSM. However, the very hostile conditions in these regions (distance from the continents, cold temperatures and low light in winter, strong storms) certainly explain why fishing effort remains very low.

South of 55°S, around the Antarctic, epipelagic fish are minor components of the HTL biomass (Rodhouse and White, 1995). This paradoxical absence of fish, despite high levels of primary production, may be explained by the region's strong seasonality. The lack of essential factors, such as light and zooplankton biomass, limits feeding opportunities for fish for half of the year, preventing them from establishing in the area—especially smaller species that cannot migrate seasonally over long distances. In the southernmost part of this region, zooplankton such as krill or salp, with their very peculiar life-cycles adapted to the seasonal advance and retreat of sea ice, replace forage fish and is the most important link between primary production and warm-blooded top predators (Barrera-Oro, 2002; Murphy et al., 2016, Atkinson et al. (2004)). Endothermic top predators such as marine mammals and seabirds are indeed dominant in high-latitude

pelagic ecosystems (and in cold coastal upwellings) because, over evolutionary timescales, they have likely outcompeted large ectothermic pelagic fish predators, which are much less efficient in cold waters (Grady et al., 2019). Alternatively, Galbraith et al. (2019) proposed that the low iron concentrations observed in this subpolar region could explain the absence of fish, particularly pelagic fish. If this explanation holds, iron limitation would have acted over evolutionary timescales, as fish cannot directly sense iron concentrations to avoid iron-poor areas. Instead, natural selection may have favoured phenotypes adapted to temperature ranges that help them avoid these iron-poor regions. For all these reasons, the minimum temperatures accessible to epipelagic communities in APECOSM do not go below 8 °Celsius, preventing them from occupying the subpolar regions of the Southern Hemisphere where they are absent.

However, comparing simulated epipelagic biomasses with these indirect fishing effort observations is not straightforward, and some limitations of this comparison must be considered. First, depending on national regulations, the vessels that must be fitted with AIS generally range from more than 10 m to more than 20 m in length. This excludes small boats and therefore small-scale fishing, but also the boats that do not activate their AIS in order to avoid detection by pirates or to fish illegally. Second, it should also be noted that fishing areas do not necessarily reflect the spatial distribution of fish, as some areas are not economically attractive due to a lower abundance of commercial species or poor accessibility. Finally, the Global fishing Watch dataset includes demersal fisheries, whereas the APECOSM model currently includes only pelagic communities and therefore only a fraction of the coastal biomass exploited by fisheries, which corresponds to the fishing effort estimated by satellite.

Tropical tuna community

Here we compare the simulated distribution of the tropical tuna community with commercial catches of skipjack and yellowfin tuna. It is important to be cautious when using catch data as a proxy for spatial distribution, as tunas may inhabit areas beyond the reach of fishing activities due to their distance from fishing bases, or may be insufficiently concentrated to ensure economic viability. Tropical tunas are found in warm waters, mainly in the tropical belt of the three oceans, with higher concentrations in the Pacific Warmpool and the Somalian upwelling in the Indian Ocean, where purse seine fleet concentrate, as shown in both the model (Fig. 7.c) and the catch data (Fig. 7.d). Both maps also show important biomass and catches in the waters north-east of the USA, off Japan and along the south-east coast of Australia, where warm waters permanently or seasonally flow into these regions through western boundary currents. In the three oceans, tropical tunas are concentrated on both sides of the equator, where they swim to feed on small epipelagic organisms transported there by the equatorial divergence. The tropical Atlantic is undersampled by purse seine fisheries, with purse seiners operating mostly in the Gulf of Guinea, mainly from Ivory Coast and Ghana, and the only purse seine fishery in the western Atlantic being very localised off Venezuela (Takyi et al., 2023; Cabello et al., 2003). There is no purse seine fishing data in the southeast Asia inner seas where small-scale fisheries are dominant but are unfortunately not fully documented in the SARDARA database.

Additionally, tropical tunas are found in the waters off the Peruvian and Mexican coasts, where significant catches of yellowfin tuna (particularly off the coast of Mexico) and skipjack tuna (especially off Peru) are made, despite the relatively cold waters off the upwellings. In APECOSM, tropical tunas are present along the Peruvian coast between April and June, coinciding with skipjack catches off Peru, when warming waters allow them to approach the upwelling to feed on the abundant macrozooplankton, in particular the red squat lobster (*Pleuroncodes planipes*) which constitutes a significant portion of their

diet (Fuller et al., 2021; Robinson et al., 2004; Yapur-Pancorvo et al., 2023).

Mesopelagic feeding tuna community

The mesopelagic feeding tuna community includes in particular big-eye tuna, which live in tropical waters where they are caught by surface fisheries with tropical tunas up to about 80 cm in length, size beyond which their daytime depth is maximal (Abascal et al., 2018). At this size they begin to develop the thermoregulatory capacity necessary to extend their distribution into temperate waters and feed at depth (Hino et al., 2019). Consequently, their modelled spatial distribution is similar to that of tropical tunas up to 80 cm, while larger fish live in temperate waters and have a wider distribution (Fig. 7.e). This modelled spatial distribution is coherent with bigeyes and swordfish catches from the SARDARA database (Fig. 7.f). Purse seine catches mainly occur in the equatorial region, where the biomass of juvenile bigeye tunas is higher, while longline catches of large bigeyes and swordfishes extend further into higher latitudes (up to about 40°N and 35°S) compared to tropical tuna fisheries. In the Pacific, a triangular shape, visible on both maps, extends from the Chilean coast through the central equatorial Pacific and back to the US coast. This shape correlates with the distribution of mesopelagic residents and OMZ signature (Fig. 2.f), indicating the importance of trophic interactions between mesopelagic feeding tunas and mesopelagic residents(Fig. 7.e.f and Fig. 6.e.f).

However, in the Eastern Pacific, particularly off the equator, there are few observed catches despite a relatively large biomass in the model. Even if there is evidence that bigeye tunas exceeding 80 cm in length are present in the equatorial eastern Pacific (Humphries et al., 2024), their concentration is likely not sufficient to attract commercial fisheries. Moreover, OMZs appear to have less effect on mesopelagic tunas in the model than suggested by the literature (Zhou et al., 2021). As mentioned above for resident mesopelagics, this might be due to a biased representation of OMZs in our PISCES simulation.

Small coastal pelagic community

The small coastal pelagic community includes mainly plankton-feeding fish that live in coastal upwelling systems where the water is cold and rich (Fig. 7.g). The Somali upwelling system is unsuitable for the development of small coastal pelagics as the water is too warm when the upwelling shuts down from September to April, with no cold water corridor for them to escape. According to Checkley et al. (2017), anchovy (*Engraulis spp.*) and sardine (*Sardinops spp.*) are associated with major sources of nitrate that fuel new primary production and LTLs (e.g. diatoms and mesozooplankton). Their main distribution hotspots are located in the most productive coastal upwellings that support very high catches. They match very well with the emergent distribution of this community in the model.

The model and observations differ in two regions : the east Pacific cold tongue and the Aghulas current retroflexion region in the southeast of South Africa. In the model, the cold tongue offers a favourable environment for this community, with suitable primary production levels and a compatible temperature range for most of the year due to NEMO-PISCES. However, the coarse resolution of the model limits its ability to capture the high plankton concentrations typical of coastal upwellings, particularly in the Humboldt and Benguela. Consequently, the model fails to produce the strong coast-to-ocean contrasts needed to retain small coastal pelagic biomass near the shore in these areas.

3.1.2. Vertical distribution: What are the different processes at stake?

Most spatial marine ecosystem models represent ecological dynamics in 2 dimensions. APECOSM, as a 3-dimensional model, allows us to understand the processes underlying the vertical distribution and diel migrations of the ecological communities considered, and how they contribute to the control of trophic interactions. By comparing the day and night vertical distributions of the six communities in our APECOSM configuration with observed acoustic profiles from the Malaspina expedition (see Section 2.4.5), we can analyse the influence

and the interplay of light, temperature, oxygen, and prey distribution on shaping the size-dependent vertical profiles of the different communities in various environments.

Light sensitivity

Light is known to be a first-order determinant of the vertical distribution of marine organisms because they need to stay within certain community-specific light intensity ranges to forage efficiently as visual predators (Puvanendran and Brown, 2002; Aksnes et al., 2017) or bioluminescent ambush feeders (Young, 1983), or because they need to stay in dark waters to avoid visual predation during resting periods (Røstad et al., 2016; Langbehn et al., 2019; Klevjer et al., 2016; Belharet et al., 2024). In APECOSM, the epipelagic communities, including small coastal pelagic, small and medium epipelagic, tropical tuna and mesopelagic feeding tuna smaller than 80 cm, are visual daytime feeders that forage in the well-lit euphotic zone of the ocean above 200 m, mainly around 50 m (Fig. 8.a, b, c, e, f). At these depths, light levels during the day allow them to hunt by sight, without being blinded by darkness or dazzled by too much sunlight. Because clear waters allow deeper light penetration, these communities follow the isolumes and tend to live deeper when the water is clear, as can be seen in Fig. 9.d: For this reason, the biomass of the epipelagic communities is deeper in the North and South Pacific oligotrophic gyres (between about 15° and 35° N and S) than in the equatorial Pacific (15°N-15°S). This is also clear from Fig. 9.b, where the epipelagic communities deepen from the "green waters" of the East Pacific Cold Tongue to the "blue waters" of the West Pacific Warm Pool, as do the isolumes.

Fishes from the mesopelagic feeding tuna community, such as big-eye tuna or swordfish, are diurnal. They have larger eyes than tropical tunas. When they acquire the thermoregulatory capabilities required to stay longer in cold mesopelagic waters (Block and Stevens, 2001; Graham and Dickson, 2004), their large spherical lenses allow them to hunt in deep waters where light levels are lower than at the surface. This size-dependent ontological shift between epipelagic feeding and mesopelagic feeding occurs at about 80 cm in the model (Fig. 8.e).

Mesopelagic communities remain in the twilight zone during the day, where they can hide from visual predators. As their visibility to predators increases with size, so does their sensitivity to light in APECOSM. It causes mesopelagic fish within the same community to live deeper as they grow, allowing them to hide from predators in darker waters when their visibility increases (Fig. 8.c, d). In the model, mesopelagic migrants are nocturnal. They are adapted to low light intensities, which they follow at night to feed on epipelagic and smaller migratory organisms at the surface, while remaining invisible to epipelagic predators (Langbehn et al., 2019).

Temperature preference

Temperature controls the horizontal distribution of fish communities, particularly for epipelagic communities that inhabit surface waters where temperature variability is greater than at depth. It also affects the vertical distribution of fish (Freitas et al., 2021). In addition to the community-specific temperature limits, that may prevent the different communities from reaching certain depths in the model, rapid variations in the core temperature of epipelagic tunas have indeed been shown to limit their vertical movements (Brill, 1998). In APECOSM, the difference in water temperature between the surface and the ambient depth is therefore considered to be a limiting factor in the vertical distribution of epipelagic communities during the night. The need to avoid sharp thermal gradients means that they mostly stay above the thermocline at night, when light does not determine their depth. This leads to a more diffuse vertical distribution of epipelagic organisms during the night than during the day, when light and the distribution of prey concentrate the biomass around 50 m depth (Fig. 8a, b, e, f). It also implies that temperate communities, such as small and medium
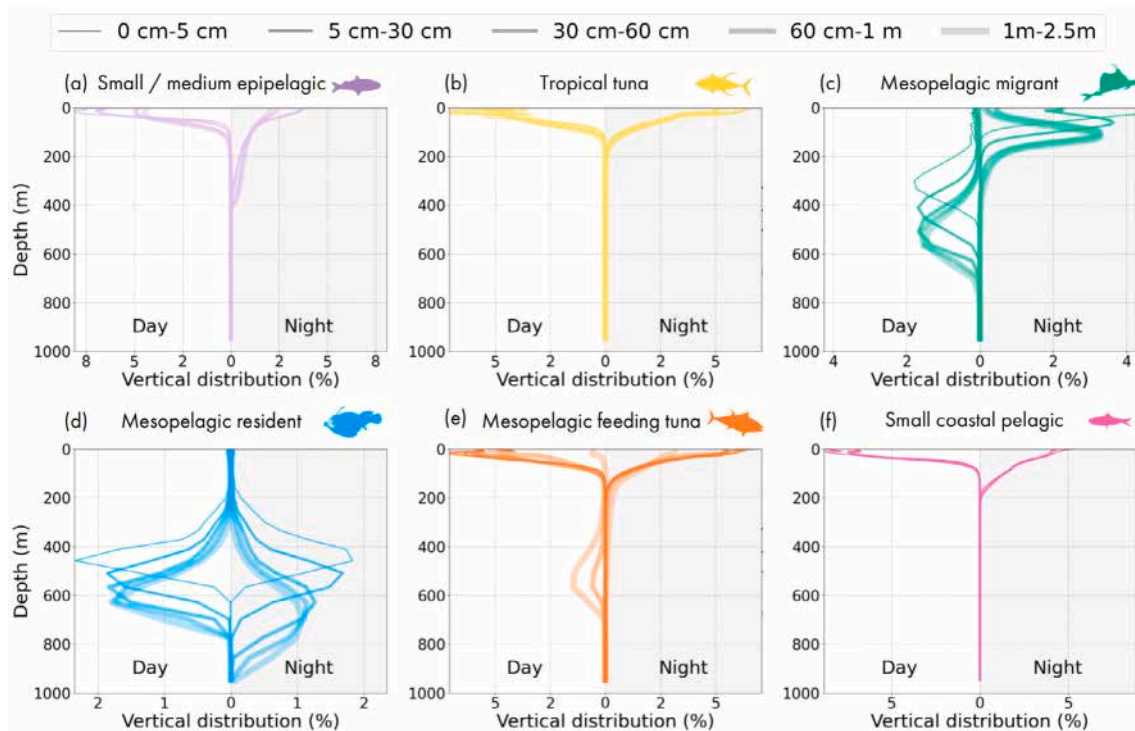
Fig. 8. Globally averaged vertical distribution for each community and for different size groups averaged over 2000–2020. The most transparent colours correspond to the smallest size groups. The values are given as percentages of the total biomass density of each size group.

epipelagic and mesopelagic feeding tunas, may descend quite deep at night, especially in the absence of a clear thermocline.

Oxygen limitation

In certain regions of the ocean such as the Eastern Tropical Pacific, the Arabian Sea, and the Bay of Bengal, the concentration of dissolved oxygen falls below the level required to support most pelagic macro-organisms. In these regions, designated as oxygen minimum zones (OMZs), oxygen concentration may drop below 1 ml/L between 200 m AND 1000 m depth. Belharet et al. (2024) described the existence in the Malaspina acoustic data of two characteristic vertical distributions of biomass inside and outside the OMZs (Section 2.4.5). During the day, the general pattern outside the OMZ regions shows stronger acoustic signals at greater depths, particularly around 500 m, corresponding to mesopelagic fish (Fig. 10.b). At night, however, the signal is stronger at the surface because of the diel vertical migration of mesopelagic migrants. In the low oxygen pattern stations, in the eastern tropical Pacific OMZ, almost all the acoustic signal below 200 m disappears at night, suggesting a weak presence of mesopelagic residents in the OMZ or organisms not resonant at 38 kHz (Fig. 10.c). In this region the mesopelagic migrant community is still present despite the low oxygen concentration but its distribution is about 150 m shallower during the day compared to the general pattern. At night, mesopelagic migrants are also shallower than in the general pattern stations, because they prey on epipelagic organisms, which are concentrated at the surface due to their high oxygen requirements. The presence of mesopelagic migrants in OMZ regions has also been described in other regions, such as the Arabian Sea (Butler et al., 2001) and the Bay of Bengal (Sutton et al., 2017).

In APECOSM, the different communities have different sensitivities to oxygen, in order to reproduce the different behaviours observed in the acoustic signal (Fig. 10). In the model, epipelagic and mesopelagic resident communities are highly sensitive to oxygen concentration, whereas mesopelagic migrants have a greater tolerance to low-oxygen waters. Epipelagic fish have therefore a more restricted vertical distribution at the surface in OMZs, making them more vulnerable to

predators, while mesopelagic feeding tunas still have the ability to hunt at depth, but for a shorter time, spending more time at the surface than in non-oxygen restricted regions, as already observed (Brill et al., 2005; Humphries et al., 2024). Mesopelagic residents, which normally inhabit depths around 500 m, would be pushed into shallower waters where oxygen levels are higher, but due to their adaptation to low light intensities, they would be dazzled by the brighter surface waters. This would render their bioluminescent traps ineffective and leave them unable to forage. As a result, mesopelagic residents are absent from the OMZs in APECOSM as in the observations (cf. Fig. 9.d, z and Fig. 10.c).

The distribution of prey

In APECOSM, the vertical distribution of prey influences the predators' location in the water column, during the day for diurnal communities and at night for the mesopelagic migrants. Small coastal pelagic, small and medium epipelagic, tropical tuna communities forage in the epipelagic zone, while mesopelagic residents feed in the mesopelagic zone. These groups only adjust their depth to optimise encounters with aggregated, visible prey (Fig. 8.a, b, d, e, f). In contrast, the mesopelagic migrant community undergoes substantial diel vertical migrations, hiding in the dark mesopelagic waters during daylight and moving in the epipelagic zone at night to access visible prey (Fig. 8.c). The pattern is reversed for the large individuals of the mesopelagic feeding tuna community, which are feeding in mesopelagic waters during the day and staying at the surface at night (Fig. 8.e). The light penetration and the plankton distribution being deeper in the gyres (Pérez et al., 2006), the epipelagic communities tend to forage deeper during the day in these regions (Fig. 9.d) as does the mesopelagic migratory community at night (Fig. 9.c, Fig. 9.e).

3.1.3. The community size spectra quantify the structural organisation of the global pelagic ecosystem

The size spectrum of marine communities, namely the distribution of their biomass across individual size classes, exhibits a remarkable degree of regularity that characterises the structure of aquatic ecosystems
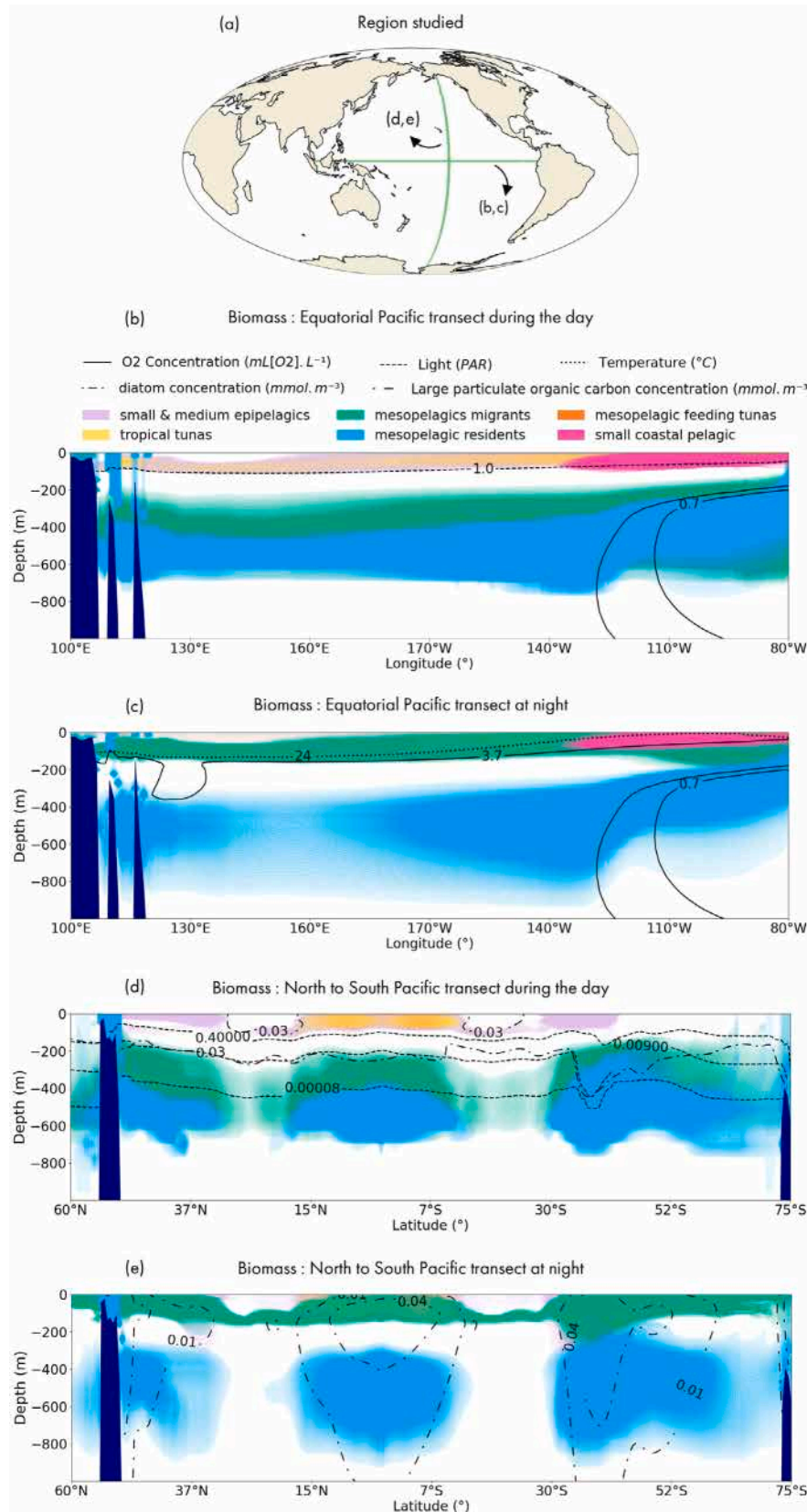
Fig. 9. Vertical distributions along two zonal and meridional transects in the Pacific. (a) represents the location of the 2 transects in the Pacific Ocean. For each community, the yearly mean size-integrated biomass is represented. The solid, dashed and dotted lines represent the contour of the key physical and biogeochemical variables that influence the vertical distribution. The equatorial transect during the day (b) and at night (c) (yearly mean). The North to South Pacific transect day (d) and night (e) (yearly mean). The biomass of communities is superimposed, with high biomass communities having greater opacity, thus hiding low biomass communities such as tropical tunas and mesopelagic feeding tunas. The latter is often represented above the tropical tuna community for better visibility.
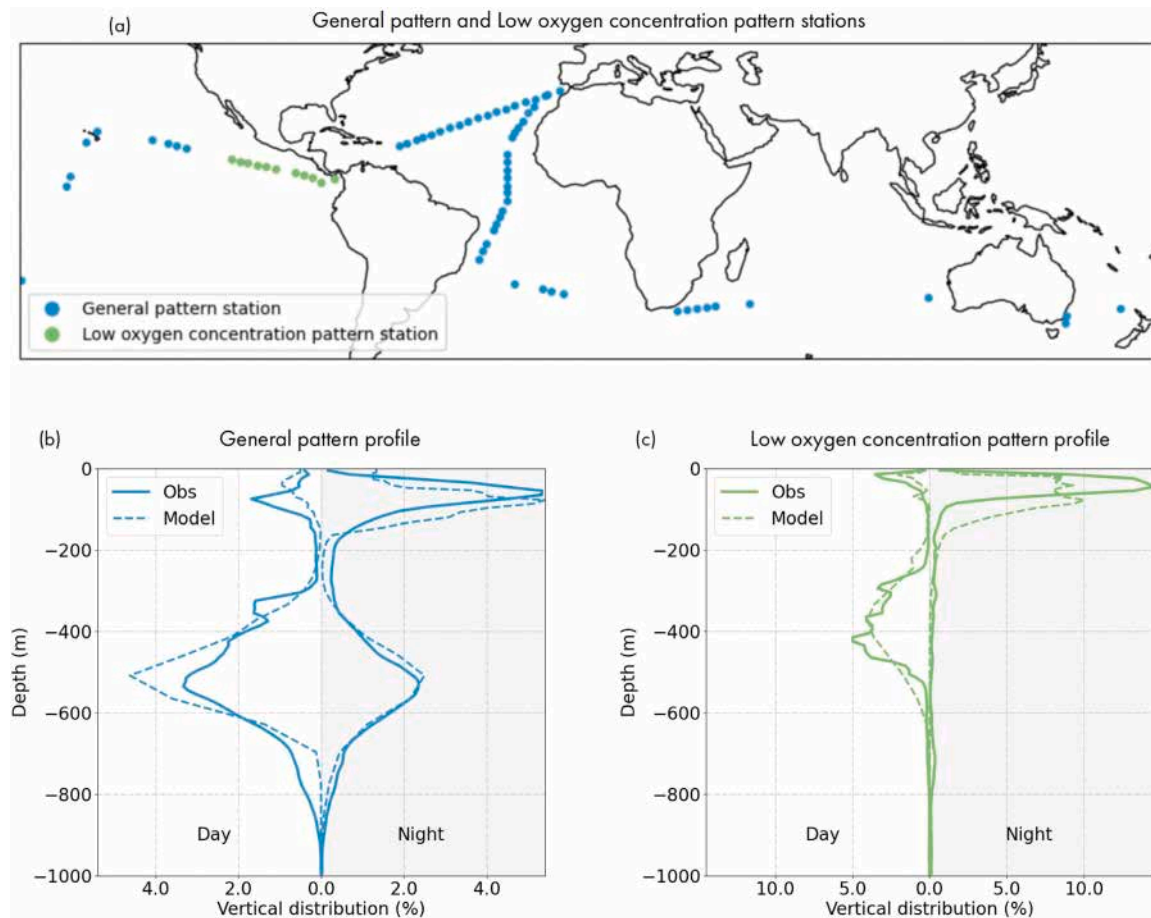
Fig. 10. Vertical distributions at the Malaspina expedition stations. The vertical profiles of the simulated biomass and the observed acoustic backscatter were extracted at each station of the Malaspina expedition and averaged in each of the two categories distinguished on the map (a) : general pattern stations in blue and OMZ stations in green. The average day and night relative vertical profiles of the acoustic signal observed during the Malaspina expedition (solid lines) and the total biomass predicted by APECOSM (dashed lines) are represented for both the general pattern stations (b) and the OMZ stations (c).

(Sheldon et al., 1972; Sprules et al., 2002; Buba et al., 2017; Hatton et al., 2021). This regularity is frequently represented by the relationship between the logarithm of numerical abundance and the logarithm of organism size, which has usually a slope approaching -1. This relationship is largely explained by the size-dependent nature of predator–prey interactions and metabolism (e.g. growth, maintenance, reproduction and mortality) (Zhou, 2006; Zhang et al., 2013; Plank, 2011, Guiet et al., 2016).

Our PISCES-APECOSM coupled model set-up is designed to include the main functional components of pelagic ecosystems in the first 1000 m of the ocean. The PISCES model provides six major LTL groups (small and large phytoplankton, i.e. flagellates and diatoms, micro- and meso-zooplankton, and small and large detritus). One macrozooplankton group is derived from the PISCES mesozooplankton. Our APECOSM configuration represents six HTL communities, including mesopelagic communities, as well as small- to large-sized epipelagic communities.

Global scale

In agreement with theoretical expectations, the modelled total biomass size-spectrum, which aggregates the biomass of the six HTL communities at the global scale, aligns fairly well with the LTL biomass size-spectra to which APECOSM sets an arbitrary -1 slope over their respective size ranges (Fig. 11.a). By integrating the global HTL biomass size spectrum over its entire size-range (e.g. 1 mm–2.5 m) (Fig. 11.a), we calculated the annual average total HTL biomass between 2000 and 2020 in APECOSM to be about 2.9 gigatonnes on a global scale.

Together, the mesopelagic communities represent 2.5 gigatonnes globally in the model, which falls in the range of previous estimates of 1.8 to 16 gigatonnes (e.g. Proud et al., 2019). The total biomass of the mesopelagic residents in the model is estimated to 1.5 gigatonnes tonnes (52% of the total simulated biomass), higher than that of mesopelagic migrants that we estimated to be 1 gigatonnes tonnes (34% of the total simulated biomass) and that of the epipelagic communities that we estimate to be 383 million tonnes in average (13% of the total simulated biomass). In the absence of global empirical estimates, we used the mean ratio of the vertically integrated acoustic signal of the epipelagic and mesopelagic communities in the circumnavigation Malaspina dataset as a proxy to assess the proportion of each APECOSM communities. In the general pattern stations (Fig. 10.a), we computed the difference between the acoustic backscatter signal at depths above 200 m at night and during the day to determine the proportion of mesopelagic migrants. For the epipelagic communities we used the acoustic data above 200 m during the day and for the mesopelagic resident community we used the acoustic signal detected at depths below 200 m during the night. The mesopelagic resident community represents 59% of the total acoustic backscatter, the mesopelagic migrant 30% and the epipelagic communities 11%. These empirical proportions confirm the orders of magnitude simulated by APECOSM, although they should be treated with caution. In particular, because of the likely underestimation of the signal from the epipelagic community and the consequent overestimation of the proportion of mesopelagic communities.

Within the epipelagic group, the small coastal pelagic and the small and medium epipelagic communities include species that can reach up to 41 cm and 84 cm respectively. Although they are more abundant than larger epipelagic fishes in the model, their total biomass is much lower than that of the mesopelagic communities. Together, the simulated epipelagic communities account for about 380 million tonnes globally. Small coastal pelagics and small and medium epipelagics account for about 180 million tonnes each. These biomass estimates are calculated by integrating over the entire size range of the different communities including small-sized larvae and juveniles that are not harvested. They therefore exceed the biomass of the corresponding fished stocks. If we consider fishable sizes only, these numbers correspond to 40 million tonnes for small coastal pelagic organisms larger than 8 cm, and 80 million tonnes for small and medium epipelagic species larger than 8 cm. The tropical tuna community includes among the largest fish predators in the epipelagic zone. Less abundant than the small and medium community, which includes smaller species, tropical tunas account for 15 million tonnes in our simulation, with skipjack and yellowfin tuna catches representing 5 million tonnes in 2019 (FAO, 2021). Mesopelagic feeding tunas, which include larger species that can reach 2.5 m in our configuration, account for an annual average of 8 million tonnes, while bigeye tuna catches represent 0.4 million tonnes in 2019 (FAO, 2021).

Indian Ocean

IOTC catch and size-frequency data have been used to reconstruct the size distribution of the catch of all the species harvested (see Section 2.4.6). These data are compared to the APECOSM biomass of tropical and mesopelagic feeding tunas simulated over the same period in the Indian Ocean (Fig. 11.b). For fishable sizes, ranging from 30 cm to about 2 m, the APECOSM size spectra show a slope of about −1 before falling down steeply, displaying a pattern similar to the IOTC catches. The two bumps in the observed catches correspond to purse seiners and, to a lesser extent, bait boats that are catching fish in schools (see Maury, 2017 for an explanation of these two modes that are not reproduced in APECOSM). Larger tunas, which are less abundant and do not school, are caught with lines and longlines (Kaplan et al., 2014). Comparing observed catches (in T over 5 years) with simulated biomass (in $T \cdot yr^{-1}$) within the same size range enables analysis of the size spectrum slope and shape. However, this approach is not directly helpful to assess the absolute biomass of the modelled tropical and deep-feeding tuna communities.

Atlantic Ocean

The data on phytoplankton, zooplankton and mesopelagic organisms compiled in the Triatlas project cover a wide range of ecological zones within the Atlantic Ocean, from upwelling regions to warm tropical waters and OMZs (see Section 2.4.7). Unlike the commercial catches used in the previous paragraph, they allow the assessment of the absolute values of the simulated size distributions. Here we compare them with PISCES and APECOSM outputs in the same areas. Overall, the modelled and observed size spectra show remarkable consistency over a range of individual weights covering 20 orders of magnitude for the model outputs and 17 for the observations. This demonstrates the ability of the coupled PISCES-APECOSM models to reproduce the alignment, slopes and intercepts (i.e. absolute levels of biomass) of the different community size-spectra, and therefore their ability to capture both the intra- and inter-community structure of the ecosystem at the ocean scale.

3.2. Emergent trophic functioning of the ecosystem

In the previous section (Section 3.1) we explored how the ecosystem structure, simulated by APECOSM in five dimensions (latitude, longitude, depth, communities, body length), emerges from the interactions between organisms and their environment, including prey and predators, and how it depends on the configuration of each community. In
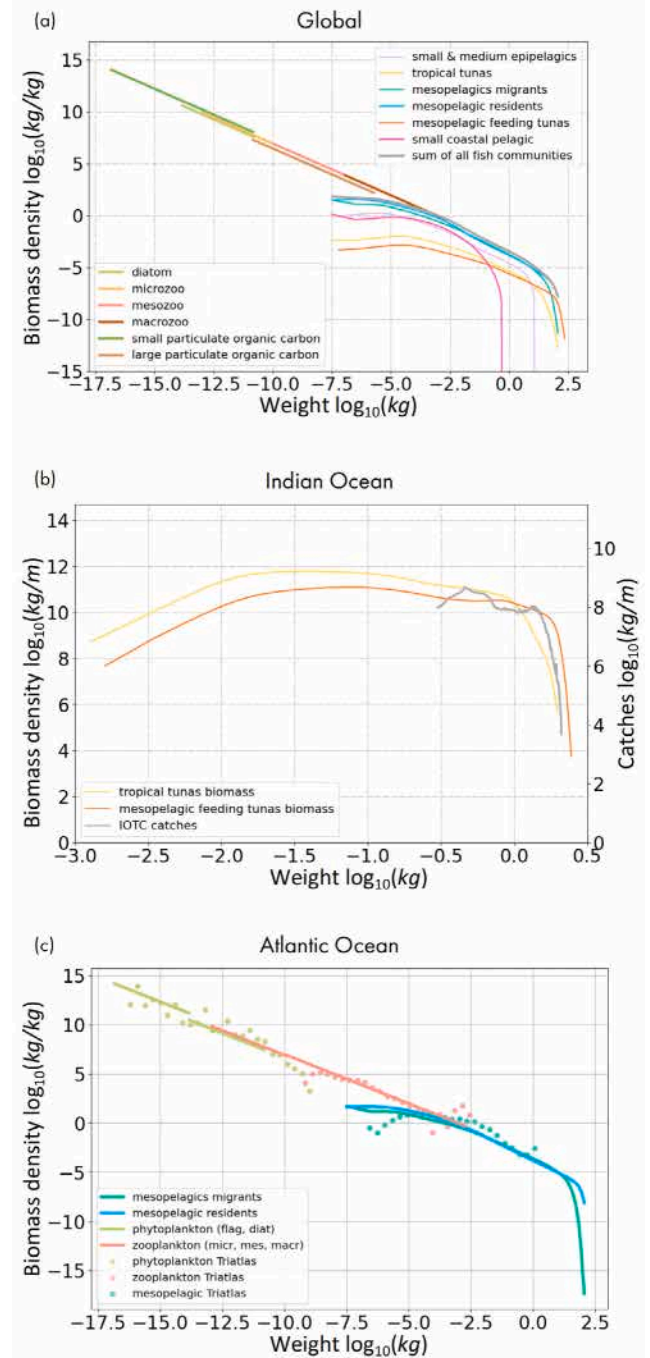
Fig. 11. Size-spectrum. Globally aggregated size spectra of the PISCES low trophic level groups (diatom, microzooplankton, mesozooplankton, small and large particulate organic carbon) that are driving APECOSM and the six high trophic level communities simulated in our APECOSM configuration. The sum of the globally averaged annual mean biomass size spectra of all the APECOSM communities aligns well with the phytoplankton, zooplankton, and particulate organic carbon (a). The mean global annual biomass of mesopelagic resident organisms is approximately 1.5 gigatonnes. The mean global annual biomass of mesopelagic migrants is approximately 1 gigatonne. Small and medium epipelagic and small coastal pelagic organisms represent about 180 million tonnes each. The respective biomass of tropical and mesopelagic-feeding tunas is approximately 15 and 8 million tonnes. The average biomass size spectra of the tropical tuna and the deep feeding tuna communities from APECOSM in the Indian Ocean are compared to the IOTC catch over 5 years by size data from the same region (see Section 2.4.6) (b). The average phytoplankton and zooplankton size-spectra simulated by PISCES as well as the resident mesopelagic and migratory mesopelagic size-spectra simulated by APECOSM in the Atlantic Ocean are compared to the corresponding observations gathered in the same region by the Triatlas project (see Section 2.4.7) (c).

this section, we examine how ecosystem functioning, and in particular trophic interactions between communities, result from this structural organisation. In APECOSM, trophic interactions are not prescribed. As illustrated in Fig. 1, communities interact through dynamic, opportunistic, and size-dependent trophic relationships. These interactions are controlled by the spatial co-occurrence of predators and prey, their size ratios, and the aggregation and visibility of prey. The diet of marine fish is indeed highly dependent on their size (Jennings et al., 2001, Butler et al., 2001; Scharf et al., 2000; Juanes, 2016), vertical behaviour (Lin et al., 2020), and the availability of different potential food components.

The epipelagic resident communities

Small coastal pelagics are microphagous planktivores, and their high abundance in upwelling systems is attributed to their ability to feed directly on plankton (Espinoza and Bertrand, 2008, Fig. 12.f). Anchovy and sardine consume phytoplankton and zooplankton by filtering particles from the water, biting individual particles, or both (van der Lingen et al., 2009). Stomach content studies show that zooplankton contributes most of the dietary carbon of sardines, with small copepods, anchovy eggs and crustacean eggs being their main prey (e.g. Van Der Lingen, 2002; Morote et al., 2010). However, while adults in the model feed mainly on mesozooplankton, the diet of their larvae is dominated by phytoplankton (Fig. 12.f). As larvae and small juveniles make up most of their biomass, the largest energy flux supporting the small coastal pelagic community is actually from large phytoplankton (Fig. 13). The high dependence of this community on the base of the food web can lead to bottom-up control, for example in the Humboldt upwelling where changes in zooplankton biomass contribute to variations in anchoveta population size (Ayón et al., 2008). Their huge biomass in upwelling regions has also been shown to be at the origin of wasp-waist control of the ecosystem (Cury et al., 2000), where small pelagics are so abundant that they simultaneously control higher (bottom-up control) and lower trophic levels (top-down control). In APECOSM, small coastal pelagics larvae first eat diatoms and microzooplankton. They then shift to mesozooplankton when they are around 1–2 cm long, and feed almost exclusively on zooplankton at 10 cm length (Fig. 12.f). In this community, as in all other APECOSM communities, the functional response of the small size classes, especially when planktonophagous, is lower compared to large size classes. This is probably due to the lower swimming speed and therefore the smaller volume of water explored.

In the model, the small and medium epipelagic community and the tropical tuna community also inhabit and forage in the epipelagic zone. When they are too small to feed on larger prey, their diet consists exclusively of mesozooplankton (60% of all epipelagic resident communities and size classes combined biomass intake in the model, Fig. 13) until they reach about 3 cm in length (Fig. 12.a,b,c,e). This is in line with established knowledge that zooplankton is the main food source for pelagic larvae (Nunn et al., 2012). As they grow, they can catch and ingest larger prey (Mittelbach and Persson, 1998). Moreover, the improvement of their swimming performance increases their search volumes (Nunn et al., 2012) and therefore the amount of prey they consume (Carvalho et al., 2002). As simulated by the model, they transition from zooplanktivory to piscivory from 2 to 5 cm (Fig. 12; Galarowicz et al., 2006), after which they start diversifying their diet and feed on every available epipelagic prey groups, including small and medium epipelagics, small coastal pelagics, small tropical tunas and small mesopelagic tunas (Fig. 12.a,b,e).

The mesopelagic resident community

Unlike most other communities in APECOSM, mesopelagic resident organisms do not forage at the surface. They therefore cannot substantially feed on the planktonic groups simulated by PISCES, which are much shallower, mostly above 200 m (Fig. 12.d). In the model, zooplankton only appears in the diet of mesopelagic resident organisms

smaller than 3.5 cm, which inhabit shallower regions than larger organisms (Fig. 8.d) and can therefore access the deep tail of the PISCES mesozooplankton vertical distribution. Several gut content analysis studies indicate the presence of zooplankton, mainly mesopelagic resident and migratory species, in the diet of mesopelagic resident fish, with a significant proportion of copepods (Thompson and Kenchington, 2017; Granata et al., 2023 ; McClain-Counts et al., 2017; Pearcy et al., 1979). However, given the absence of mesozooplankton below 200 m and the absence of vertical migrations of LTLs in PISCES (Burd et al., 2010 but see Gorgues et al., 2019), the diet of small mesopelagic residents in APECOSM is mainly composed of particulate organic carbon, with a very marginal presence of zooplankton, which may explain the lower functional response of small mesopelagic residents compared to other communities (Fig. 12.d) (the scaled functional response measures the degree of satiation, it varies from 0 -no food consumption- to 1 -satiation-). While zooplankton may be significantly underestimated in the diet of mesopelagic resident organisms simulated by APECOSM, the importance of large organic particles in their simulated food is interesting. Marine snow is indeed a naturally occurring macroscopic aggregation of suspended particles composed of detritus, faeces and carcasses of dead animals, partly decomposed by bacteria and ciliates. It is an almost universal component of suspended matter in the ocean (Alldredge and Silver, 1988), and recent dietary studies, frequently employing isotopic analyses, have shown that small mesopelagic resident fishes are highly dependent on marine snow, with this dependence intensifying with depth (Valls Mir et al., 2014; Badouvas et al., 2024; Gloeckler et al., 2018; Tsukamoto and Miller, 2021). These studies suggest that POM plays a pivotal role in sustaining the organisms inhabiting the depths, where resources are otherwise scarce. Its availability may have a significant influence on biological processes across a vast expanse of the deep sea (Smith et al., 1997 ; Smith et al., 2008 ; Smith and Demopoulos, 2003). They thus confirm the predictions of APECOSM that marine snow is a major component of the diet of small mesopelagic resident organisms and is therefore necessary for the maintenance of their entire community. As they grow, mesopelagic organisms gain access to larger prey (Choy et al., 2013; Valls Mir et al., 2014). In APECOSM, they feed exclusively on mesopelagic migrants and themselves, with a higher proportion of food from their own community when they are over 7–8 cm long (Fig. 12.d). This is due to the greater abundance of the resident community compared to the migratory community in our simulation (Section 3.1.3), but also to the difference in their depths, with the migrants living slightly shallower than the residents (Fig. 9.b, d), especially the migratory prey that are much smaller than their resident predators (Fig. 8.c and d) thus keeping a fraction of their community inaccessible to the mesopelagic residents.

The migratory communities

Small migratory mesopelagic organisms feed mainly on zooplankton such as small copepods and other crustaceans, gelatinous organisms and larvae (Bernal et al., 2015; Gordon et al., 1985). The emergent diet of the migratory community in APECOSM reflects these observations, with mesopelagic migrants feeding predominantly on mesozooplankton and macrozooplankton until they reach a length of about 10 cm. They then shift to a predominantly nektonic diet at about 20 cm in length (Fig. 12.c). Beyond this length, the simulated mesopelagic migrants feed mainly on their own community, and more marginally on epipelagic fish and macrozooplankton. This is corroborated by observational studies, which show that despite their diel foraging migrations to the epipelagic zone, a large proportion of the diet of large mesopelagic migrants actually consists (and increasingly so with predator size) of organisms belonging to their own migratory community, including fish, cephalopods, crustaceans and gelatinous organisms, and only secondarily of epipelagic fish (e.g. Bernal et al., 2015; Choy et al., 2013; Riaz et al., 2020). According to Choy et al. (2013), cannibalism of small juveniles can account for up to 40% of the diet of large mesopelagic top predators such as large lancetfish (*Alepisaurus ferox*) over 120 cm.
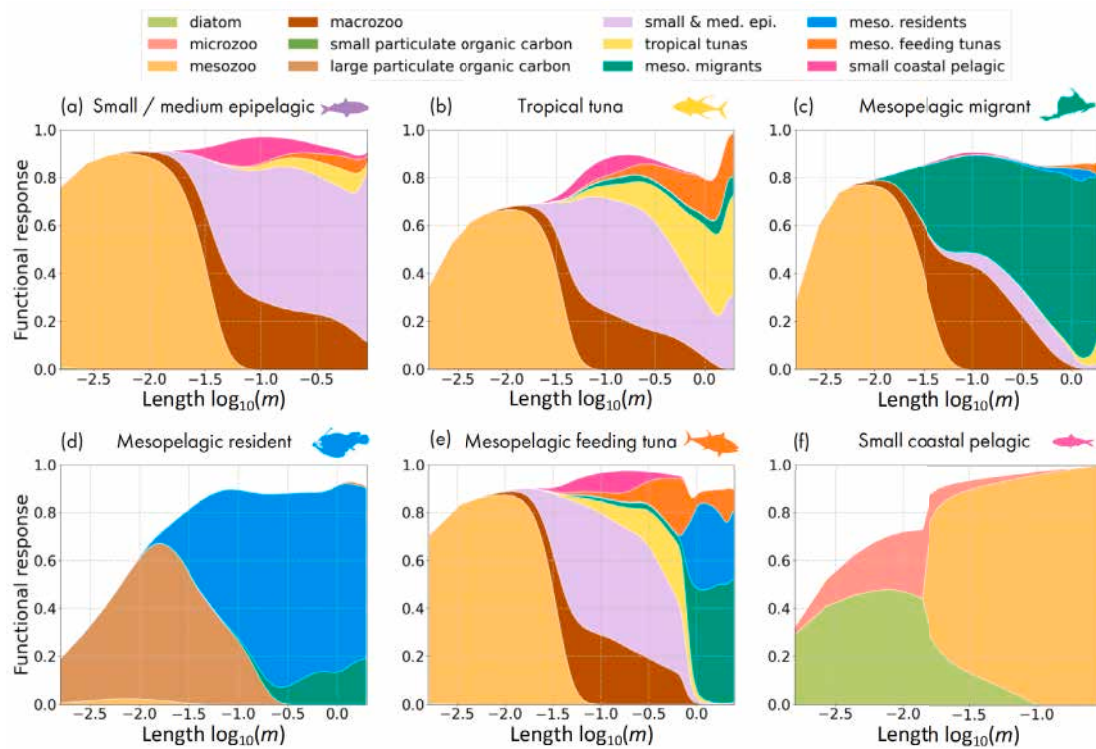
Fig. 12. Average global community diets. Community diets represent the relative proportions of the different food components of an individual predator of a given size and community, relative to satiation (satiation occurs when the functional response equals 1). The diet depends on the spatial (3D) co-occurrence between predator and prey, their size ratio, and the aggregation (schooling) and visibility of the prey.
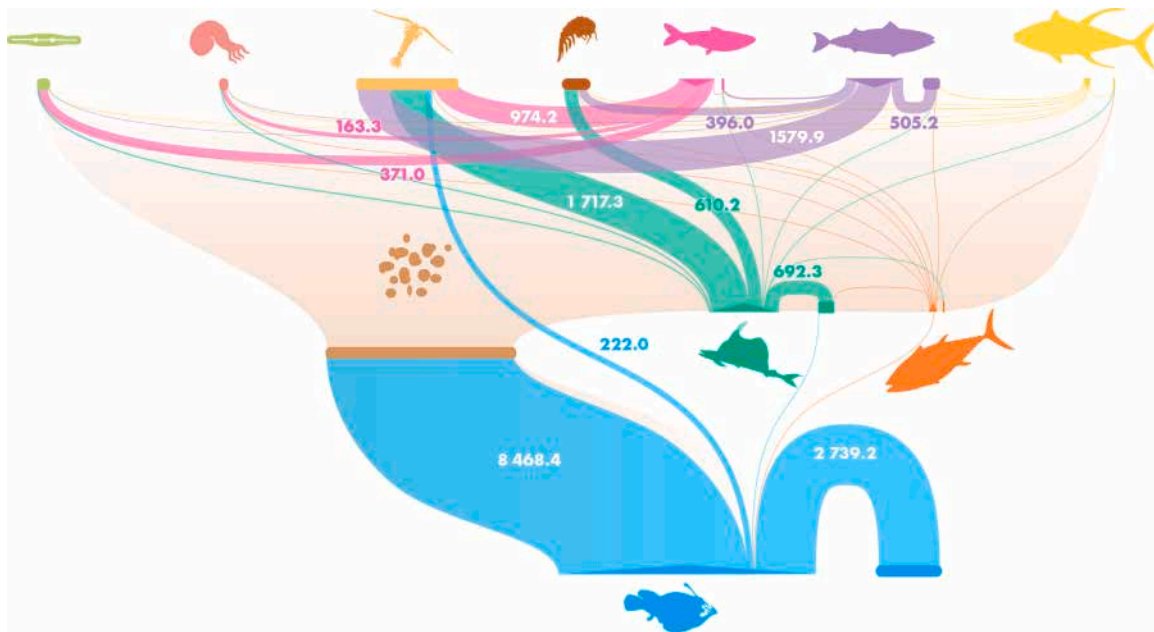
Fig. 13. Trophic interactions fluxes in $\mathrm{kton \cdot year^{-1}}$. The absolute fluxes of biomass (global average from 2000 to 2020) that are actually transferred through trophic interactions between the different communities, all sizes included, provide an integrative picture of ecosystem functioning. The fluxes connect the prey to the predator. Their colours correspond to the predators and their width is proportional to the absolute value of the flux. As small sized predators are the most abundant in the ecosystem, the trophic fluxes from plankton and particulate organic matter, which constitute most of their prey, dominate the system. The largest fluxes couple the epipelagic and the mesopelagic realms together, with the mesopelagic resident community feeding on particulate organic matter, and the mesopelagic migrant community feeding on mesozooplankton. Values shown represent fluxes $\geq 100\mathrm{kton \cdot year^{-1}}$.

APECOSM reproduces this high proportion of migratory mesopelagic organisms in their diet and explains it by their much higher abundance compared to epipelagic prey. As predation is opportunistic in the model, their emergent diet reflects the relative importance of the communities present in epipelagic waters at night, and their size-dependent availability (aggregation, visibility and size) to predators.

The simulated diet of the mesopelagic feeding tuna community exhibits the most complex pattern (Fig. 12.e). As juveniles, the organisms of this community inhabit the epipelagic zone where they feed during the day (Fernández-Corredor et al., 2023). This is consistent with trophic studies showing that juvenile bigeyes have a diet similar to tropical tunas in terms of prey taxonomy and diversity, although the proportions may vary depending on the region (Potier et al., 2004; da Silva et al., 2019). As they grow, mesopelagic tunas change their diet, when they acquire the physiological ability to hunt at depth (Lin et al., 2020; Holland et al., 2003) where preys are more abundant (Fig. 9.b, d). Observations (e.g. Ohshimo et al., 2018; Potier et al., 2004; Fernández-Corredor et al., 2023) show that mesopelagic feeding tunas over 1 m in length feed primarily on mesopelagic squid and fish. This dietary shift, which occurs in APECOSM between 60 cm and 1 m (Fig. 12.e), allows this community to reduce competition with other epipelagic fishes and thus coexist in a resource-limited oligotrophic pelagic system (Varela et al., 2023).

Trophic coupling between the epipelagic and the mesopelagic realms

Our analysis of the community diets shows that pelagic ecosystems, which are highly vertically structured, host clearly distinct epipelagic (Fig. 12.a,b,f) and mesopelagic (Fig. 12.d) food webs. However, it also shows that these food webs are not independent and that they are connected by numerous trophic linkages that transfer matter and energy from the epipelagic domain to the mesopelagic domain and conversely (Fig. 12.c,e). The community diets represent the proportions of the different food components of an individual predator of a given size and a given community, relative to consumption rate. Since community biomass decreases very strongly with size (Fig. 11), it is useful to complement the analysis of diets with the analysis of the absolute fluxes of biomass that are actually transferred through trophic interactions between the different communities, all sizes included (Fig. 13). When examining these absolute biomass fluxes in APECOSM, the fundamental role of particulate organic matter in the epipelagic–mesopelagic coupling is obvious. In the model, the flux of marine snow (the large organic particles simulated by PISCES, which in the ocean originates from the faeces of epipelagic organisms and their carcasses) is ingested by the resident mesopelagic community. It represents 74% of their total ingestion rate and 45% of the total feeding flux of all pelagic HTL communities and size classes combined. In our simulation (which, however, most likely underestimates the role of migrating zooplankton), this descendant organic matter flux represents the essential part of the diet of the small mesopelagic resident organisms (Fig. 12.d). Without it, these small organisms could not survive and this community could not be maintained in the model.

The mesopelagic migrant community is also responsible for a major transfer of organic matter from the epipelagic domain, where it feeds, to the mesopelagic domain, generating a significant descendant biomass flux (13% of the total trophic fluxes in the model, all communities and size classes combined), with predation on epipelagic mesozooplankton and, to a lesser extent, on macrozooplankton accounting for 9% and 3.2% of this flux respectively (absolute fluxes are provided Fig. 13).

Finally, the case of organisms from the mesopelagic feeding tuna community is interesting because they feed on mesopelagic communities for a large part of their life cycle and are therefore responsible for an ascendant flux of energy from the mesopelagic realm to the epipelagic realm, where they reproduce and produce faeces, although they are not subject to much predation due to their large size. These interactions between different layers play an essential role in the functioning of marine ecosystems. They connect the different trophic levels, the vertical domains and the horizontal regions (through movements and migrations) of the ocean together, thus stabilising the dynamics of the entire system. They regulate energy and material flows (Bollens et al., 2011; Bertrand et al., 2011) and allow the transfer of biomass

from the surface layers, where most of the primary production occurs, to remote mesopelagic consumers, which inhabit cold and inhospitable regions of the ocean with no primary production, and yet have the highest biomass in the pelagic world, almost 6.5 times higher than the epipelagic biomass in our simulations (Dişa et al., 2024).

4. Conclusion

4.1. To recap

The objective of this paper is to investigate the processes underpinning the global-scale structure and trophic functioning of pelagic ecosystems, by analysing a simulation of the mechanistic model APECOSM. To ensure the relevance of the model's results, we compared them with available observations, empirical models, and existing literature. This comparison demonstrates the ability of the model to represent the pelagic ecosystem structure on a global scale, and sheds light on how it responds to key physical and biogeochemical factors, including currents, temperature, primary production, oxygen, and light. The horizontal distribution of epipelagic communities is primarily shaped by sea temperature, food and currents. In contrast, mesopelagic communities have a broader distribution in productive regions and show a strong response to the OMZ. An analysis of vertical distributions stresses the importance of light and reveals that mesopelagic residents are less abundant under low oxygen conditions, while mesopelagic migrants benefit from these environments due to reduced predation and the concentration of epipelagic prey near the surface. Across communities, the abundance of organisms follows a size spectrum with a slope of about -1, with larger organisms being less abundant than smaller ones. On a global scale, mesopelagic organisms have six to seven times more biomass than epipelagic communities, while groups containing only large species such as tuna are the least abundant.

Our mechanistic approach also helps to improve our understanding of ecological interactions between communities, and how they arise from ecosystem structure. It reveals in particular how trophic interactions are controlled by the 3-dimensional structure of biotic and abiotic factors, and how they change as individuals grow and gain access to larger or deeper prey. Finally, our analysis highlights the interdependence of the different communities considered, including the quantitative importance of the links between epipelagic and mesopelagic ones, and the key role of plankton and POM in supporting HTLs.

4.2. Limitations

Our results provide a comprehensive overview of the contemporary global pelagic ecosystem and show a strong similarity between APECOSM outputs and observations. However, both the model and the observations have inherent limitations and uncertainties that affect their accuracy and reliability. APECOSM is configured based on existing knowledge and available information, which is inherently limited and unevenly distributed across the communities considered. This imbalance is not due to differences in ecological importance but rather to differences in the ease of observation and commercial importance. For example, our understanding of mesopelagic communities — in terms of life history, physiology, diet, and migratory behaviour — remains quite incomplete, especially in under-sampled regions (e.g. St. John et al., 2016; Martin et al., 2020). This contrasts with epipelagic communities like tuna and small coastal pelagics, which have been extensively studied due to their commercial importance. In addition, both the fishing data and the acoustic observations used to evaluate the model, are inherently uncertain and biased. For example, the spatial distribution of fishing activity reflects profitable areas rather than the actual distribution of fish populations, and acoustic data are highly dependent of the frequency used and the type of organisms present, thus limiting their scope.

APECOSM, as a global ocean ecosystem model, also faces many limitations. Its low horizontal resolution limits its ability to accurately represent the specificities of coastal ecosystems, making it difficult to accurately model the ecological processes affecting small coastal pelagic communities. In addition, our macrozooplankton group is currently simply derived from the mesozooplankton simulated by PISCES. However, the zooplankton from PISCES does not extend below 200 m, whereas mesopelagic resident and migratory zooplankton are observed in the mesopelagic resident stomachs (McClain-Counts et al., 2017; Pearcy et al., 1979). Adding epipelagic, mesopelagic resident and migratory mesozooplankton and macrozooplankton communities to the model could therefore improve the representation of the simulated diet of the mesopelagic resident and deep feeding tuna communities, improve their spatial distribution and cascading impacts on migratory mesopelagics and thus on epipelagic groups.

4.3. Perspectives

Despite these challenges, APECOSM has proven to be useful for studying the structure of ecosystem and the trophic interactions in the global pelagic ocean holistically, corroborating available observations and suggesting explanations for observed patterns. Its mechanistic underpinnings provide a deeper understanding of global marine ecosystems structuring and functioning than empirical models, allowing the identification of processes responsible for biomass distribution and establishing links between ecosystem properties and community responses. The 3D modelling of various communities, from epipelagic to mesopelagic zones, and their size-structured representation are crucial for conducting detailed mechanistic ecosystem studies, which remain underrepresented in global marine ecosystem models. A cross-regional comparative analysis of how the average global structure and functioning of pelagic ecosystems is modulated by regional environments would be an interesting extension of the present study. It would help to understand the roles of seasonal variability and community-specific responses, and provide insights into how ecosystems are shaped regionally, and how key processes in one region may become secondary in another.

While APECOSM has been used to simulate and understand the processes driving the evolution of marine ecosystems in response to inter-annual variability such as ENSO (Barrier et al., 2023) and long-term climate change (Lefort et al., 2015), the new configuration of the model presented here would permit to go one step further in understanding the effects and underlying processes of marine heatwaves and climate change. In particular, it would help to identify the dominant stressors affecting each community and study how these factors influence the structure and functioning of the entire pelagic ecosystem.

Finally, our analysis is based on a one-way version of the LTL (PISCES) - HTL (APECOSM) coupling. This coupling means that mass is not conserved at the PISCES-APECOSM scale (i.e. HTL organisms in APECOSM could eat more — or less — LTLs than what is produced in PISCES) and that there is no density-dependent control of HTLs by the plankton resource, even if there is still competition between the different APECOSM communities as long as they do not feed on plankton. To overcome these limitations, our analysis could be extended to a 2-way coupling, as already attempted in Aumont et al. (2018) and Dupont et al. (2022).

CRediT authorship contribution statement

Laureline Dalaut: Writing – original draft, Visualization, Software, Investigation, Formal analysis, Conceptualization. **Nicolas Barrier:** Software, Data curation. **Matthieu Lengaigne:** Writing – review & editing, Supervision. **Jonathan Rault:** Software, Investigation. **Alejandro Ariza:** Writing – review & editing, Data curation. **Adrien Brunel:** Writing – review & editing, Data curation. **Ralf Schwamborn:** Writing – review & editing, Data curation. **Mariana Travassos-Tolotti:** Writing – review & editing, Data curation. **Olivier Maury:** Writing – review & editing, Validation, Supervision, Software, Methodology, Investigation, Conceptualization.

Declaration of competing interest

The authors declare the following financial interests/personal relationships which may be considered as potential competing interests: Laureline Dalaut reports financial support was provided by Programme Prioritaire de Recherche Océan et Climat. Mariana Travassos-Tolotti reports was provided by France Filière Pêche. If there are other authors, they declare that they have no known competing financial interests or personal relationships that could have appeared to influence the work reported in this paper.

Appendix A. Macrozooplankton implementation

The macrozooplankton community has been added in APECOSM based on the PISCES mesozooplankton.

$$\text{mesozoo} = a \int_{w_1}^{w_2} w^{-1} dw = a \ln\left(\frac{w_2}{w_1}\right) \tag{1}$$

where w_1 and w_2 are the minimum and maximum weight limits for mesozooplankton.

$$\Rightarrow a = \frac{\text{mesozoo}}{\ln\left(\frac{w_2}{w_1}\right)} \tag{2}$$

$$\Rightarrow \text{mesozoo}(w) = \frac{\text{mesozoo}}{\ln\left(\frac{w_2}{w_1}\right)} w^{-1} \tag{3}$$

$$\text{macrozoo} = a \int_{w_3}^{w_4} w^{-1} dw = \frac{\text{mesozoo}}{\ln\left(\frac{w_2}{w_1}\right)} \ln\left(\frac{w_3}{w_4}\right) \tag{4}$$

where w_3 and w_4 are the macrozoo's minimum and maximum weight limits.

Appendix B. Parameters related to community configuration

Parameters related to Fig. 5 and Appendix C (see Tables 1 and 2).

Appendix C. Equations related to the configuration of communities

Equations related to Fig. 5 (see Table 3).

Appendix D. Supplementary data

Aggregated output data and python scripts used for the figure are available online at: 10.5281/zenodo.15084427

Table 1

Table of parameters and their corresponding symbols and units.

Parameter name	Symbol	Unit
Mean error of eye response to light	Q_{opt}	W m^{-2}
Standard error of eye response to light	σ_Q	W m^{-2}
Min size-selectivity gradient	α_1	/
Max size-selectivity gradient	α_2	/
Min size-selectivity ratio	ρ_1	/
Max size-selectivity ratio	ρ_2	/
Low temperature limit	T_{inf}	K
High temperature limit	T_{sup}	K
Flatness of sigmoidal response to O$_2$	O_{2resp}	/
Threshold of O$_2$	O_{2lim}	mL O$_2$ L^{-1}

Table 2

Parameter values for each community. c0 represents the small and medium epipelagic community, c1 represents the tropical tuna, c2 represents the mesopelagic migrant, c3 represents the mesopelagic resident, c4 represents the mesopelagic feeding2 tuna, c5 represents the small coastal pelagic community.

Parameters	c0	c1	c2	c3	c4	c5
Q_{opt}	5.E2	5.E2	2.E-3	6.E-5	2.E-3	5.E2
σ_Q	1.2E3	1.2E3	2.8E−2	7.E-4	2.8E−2	1.2E3
α_1	3.	3.	3.	3.	3.	3.
α_2	0.2	0.2	0.2	0.2	0.2	0.2
ρ_1	2.5	2.5	2.5	2.5	2.5	75.
ρ_2	10.	10.	10.	10.	10.	1000.
T_{inf}	281.15	291.15	293.15	293.15	288.15	285.15
T_{sup}	304.15	305.15	304.15	304.15	303.15	294.15
O_{2resp}	10	10	10	10	10	10
O_{2lim}	1.	1.	.95	.7	.7	1.

Table 3

Configuration equations. D_{frac} is the fraction of daylight within a day, $nfactor$ is equal to 1 during the day and 10^{-6} at night. Q_{PAR} is the photosynthetically available radiation in W m^{-2}, T is the temperature in K, O$_2$ is the O$_2$ concentration is mL O$_2$ L^{-1}.

Variable	Formulation
Maximum species size	Maury and Poggiale, 2013
Light preference	$LightPref_c = \left(D_{\text{frac}} \cdot e^{\mu_c} - \frac{\sigma_c^2}{\text{nfactor} \cdot Q_{PAR}}\right) \cdot e^{\sigma_c^4 - \frac{\left(\ln\left(\frac{D_{\text{frac}}}{\text{nfactor} \cdot Q_{PAR}}\right)\mu_c\right)^2}{\sigma_c^2}}$ with: $\sigma_c^2 = \ln\left(1 + \frac{\ln(\sigma_{Q,c}^2)}{Q_{\text{opt},c}^2}\right)$ and: $\mu_c = \ln(Q_{\text{opt},c}) - 0.5 \cdot \ln(1 + \sigma_c^2)$
Day/night feeding behaviour	On/off button
Prey size selectivity	$PreySelectiv_c = \left(\frac{1}{1+e^{\alpha_1(\rho_1-R)}}\right) \cdot \left(1 - \frac{1}{1+e^{\alpha_2(\rho_2-R)}}\right)$ with: $R = \frac{L_{\text{prey}}}{L_{\text{pred}}}$
Temperature limits	$TempPref_c = \frac{1}{1+e^{\frac{T_{\lim,c}}{T} - \frac{T_{\lim,c}}{T_{\inf,c}}}} \cdot \frac{1}{1+e^{\frac{T_{\lim,c}}{T_{\sup,c}} - \frac{T_{\lim,c}}{T}}}$
Oxygen preference	$O_2Pref_c = \left(\frac{1}{1+e^{O_{2resp,c} \cdot (O_{2lim,c} - O_2)}}\right)$

Data availability

Data will be made available on request.

References

Abascal, F.J., Peatman, T., Leroy, B., Nicol, S., Schaefer, K., Fuller, D.W., Hampton, J., 2018. Spatiotemporal variability in bigeye vertical distribution in the Pacific Ocean. Fish. Res. 204, 371–379. http://dx.doi.org/10.1016/j.fishres.2018.03.013.

Aksnes, D., Røstad, A., Kaartvedt, S., Martinez, U., Duarte, C., Irigoien, X., 2017. Light penetration structures the deep acoustic scattering layers in the global ocean. Sci. Adv. 3, http://dx.doi.org/10.1126/sciadv.1602468.

Alcaraz, M., 1997. Patterns in the Ocean. Ocean Processes and Marine Population Dynamics. Consejo Superior de Investigaciones Científicas (España).

Alldredge, A.L., Silver, M.W., 1988. Characteristics, dynamics and significance of marine snow. Prog. Oceanogr. 20 (1), 41–82. http://dx.doi.org/10.1016/0079-6611(88)90053-5.

Andrade, H.A., 2003. The relationship between the skipjack tuna (Katsuwonus pelamis) Fishery and seasonal temperature variability in the south-western Atlantic. Fisheries Oceanography 12 (1), 10–18. http://dx.doi.org/10.1046/j.1365-2419.2003.00220.x.

Appeltans, W., Ahyong, S.T., Anderson, G., Angel, M.V., Artois, T., Bailly, N., Bamber, R., Barber, A., Bartsch, I., Berta, A., Błażewicz-Paszkowycz, M., Bock, P., Boxshall, G., Boyko, C.B., Brandão, S.N., Bray, R.A., Bruce, N.L., Cairns, S.D., Chan, T.-Y., Cheng, L., Collins, A.G., Cribb, T., Curini-Galletti, M., Dahdouh-Guebas, F., Davie, P.J.F., Dawson, M.N., De Clerck, O., Decock, W., De Grave, S., de Voogd, N.J., Domning, D.P., Emig, C.C., Erséus, C., Eschmeyer, W., Fauchald, K., Fautin, D.G., Feist, S.W., Fransen, C.H.J.M., Furuya, H., Garcia-Alvarez, O., Gerken, S., Gibson, D., Gittenberger, A., Gofas, S., Gómez-Daglio, L., Gordon, D.P., Guiry, M.D., Hernandez, F., Hoeksema, B.W., Hopcroft, R.R., Jaume, D., Kirk, P., Koedam, N., Koenemann, S., Kolb, J.B., Kristensen, R.M., Kroh, A., Lambert, G., Lazarus, D.B., Lemaitre, R., Longshaw, M., Lowry, J., Macpherson, E., Madin, L.P., Mah, C., Mapstone, G., McLaughlin, P.A., Mees, J., Meland, K., Messing, C.G., Mills, C.E., Molodtsova, T.N., Mooi, R., Neuhaus, B., Ng, P.K.L., Nielsen, C., Norenburg, J., Opresko, D.M., Osawa, M., Paulay, G., Perrin, W., Pilger, J.F., Poore, G.C.B., Pugh, P., Read, G.B., Reimer, J.D., Rius, M., Rocha, R.M., Saiz-Salinas, J.I., Scarabino, V., Schierwater, B., Schmidt-Rhaesa, A., Schnabel, K.E., Schotte, M., Schuchert, P., Schwabe, E., Segers, H., Self-Sullivan, C., Shenkar, N., Siegel, V., Sterrer, W., Stöhr, S., Swalla, B., Tasker, M.L., Thuesen, E.V., Timm, T., Todaro, M.A., Turon, X., Tyler, S., Uetz, P., van der Land, J., Vanhoorne, B., van Ofwegen, L.P., van Soest, R.W.M., Vanaverbeke, J., Walker-Smith, G., Walter, T.C., Warren, A., Williams, G.C., Wilson, S.P., Costello, M.J., 2012. The magnitude of global marine species diversity. Curr. Biol. 22 (23), 2189–2202. http://dx.doi.org/

10.1016/j.cub.2012.09.036.

Ariza, A., Lengaigne, M., Menkes, C., Lebourges-Dhaussy, A., Receveur, A., Gorgues, T., Habasque, J., Gutiérrez, M., Maury, O., Bertrand, A., 2022. Global decline of pelagic fauna in a warmer ocean. Nat. Clim. Chang. 12 (10), 928–934. http://dx.doi.org/10.1038/s41558-022-01479-2.

Atkinson, A., Siegel, V., Pakhomov, E., Rothery, P., 2004. Long-term decline in krill stock and increase in salps within the Southern Ocean. Nature 432 (7013), 100–103. http://dx.doi.org/10.1038/nature02996.

Aumont, O., Ethé, C., Tagliabue, A., Bopp, L., Gehlen, M., 2015. PISCES-v2: An ocean biogeochemical model for carbon and ecosystem studies. Geosci. Model. Dev. 8 (8), 2465–2513. http://dx.doi.org/10.5194/gmd-8-2465-2015.

Aumont, O., Maury, O., Lefort, S., Bopp, L., 2018. Evaluating the potential impacts of the diurnal vertical migration by marine organisms on marine biogeochemistry. Glob. Biogeochem. Cycles 32 (11), 1622–1643. http://dx.doi.org/10.1029/2018GB005886.

Ayón, P., Swartzman, G., Bertrand, A., Gutiérrez, M., Bertrand, S., 2008. Zooplankton and forage fish species off Peru: Large-scale bottom-up forcing and local-scale depletion. Prog. Oceanogr. 79, 208–214. http://dx.doi.org/10.1016/j.pocean.2008.10.023.

Badouvas, N., Tsagarakis, K., Somarakis, S., Karachle, P.K., 2024. Feeding habits and prey composition of six mesopelagic fish species from an isolated central mediterranean basin. Fishes 9 (7), 277. http://dx.doi.org/10.3390/fishes9070277.

Bakun, A., 1998. Ocean triads and radical interdecadal variation: Bane and boon to scientific Fisheries management. In: Pitcher, T.J., Pauly, D., Hart, P.J.B. (Eds.), Reinventing Fisheries Management. Springer Netherlands, Dordrecht, pp. 331–358. http://dx.doi.org/10.1007/978-94-011-4433-9_25.

Barnier, B., Madec, G., Penduff, T., Molines, J.-M., Tréguier, A.-M., Le Sommer, J., Beckmann, A., Biastoch, A., Böning, C.W., Dengg, J., Derval, C., Durand, E., Gulev, S.K., Rémy, E., Talandier, C., Theetten, S., Maltrud, M., Mcclean, J., de Cuevas, B.A., 2006. Impact of partial steps and momentum advection schemes in a global ocean circulation model at eddy-permitting resolution. Ocean. Dyn. 56 (5–6), 543–567. http://dx.doi.org/10.1007/s10236-006-0082-1.

Barrera-Oro, E., 2002. The role of fish in the Antarctic marine food web: Differences between inshore and offshore waters in the southern Scotia Arc and west Antarctic Peninsula. Antarct. Sci. 14 (4), 293–309. http://dx.doi.org/10.1017/S0954102002000111.

Barrier, N., Lengaigne, M., Rault, J., Person, R., Ethé, C., Aumont, O., Maury, O., 2023. Mechanisms underlying the epipelagic ecosystem response to ENSO in the equatorial Pacific ocean. Prog. Oceanogr. 213, 103002. http://dx.doi.org/10.1016/j.pocean.2023.103002.

Belharet, M., Lengaigne, M., Barrier, N., Brierley, A., Irigoien, X., Proud, R., Maury, O., 2024. What determines the vertical structuring of pelagic ecosystems in the global ocean?. http://dx.doi.org/10.1101/2024.07.04.602098.

Bernal, A., Olivar, M.P., Maynou, F., Fernández de Puelles, M.L., 2015. Diet and feeding strategies of mesopelagic fishes in the western Mediterranean. Prog. Oceanogr. 135, 1–17. http://dx.doi.org/10.1016/j.pocean.2015.03.005.

Bertrand, A., Ballón, M., Chaigneau, A., 2010. Acoustic observation of living organisms reveals the upper limit of the oxygen minimum zone. PLOS ONE 5 (4), e10330. http://dx.doi.org/10.1371/journal.pone.0010330.

Bertrand, A., Chaigneau, A., Peraltilla, S., Ledesma, J., Graco, M., Monetti, F., Chavez, F.P., 2011. Oxygen: A fundamental property regulating pelagic ecosystem structure in the coastal southeastern tropical pacific. PLOS ONE 6 (12), e29558. http://dx.doi.org/10.1371/journal.pone.0029558.

Blanchard, J.L., Novaglio, C., Maury, O., Harrison, C.S., Petrik, C.M., Arcos, L.D.F., Ortega-Cisneros, K., Bryndum-Buchholz, A., Eddy, T., Heneghan, R., Roberts, K.E., Schewe, J., Bianchi, D., Guiet, J., van Denderen, D., Palacios-Abrantes, J., Liu, X., Stock, C.A.A., Rousseau, Y., Büchner, M., Adekoya, E., Cheung, W., Christensen, V., Coll, M., Capitani, L., Datta, S., Fulton, B., Fuster, A., Garza, V., Lengaigne, M., Lindmark, M., Murphy, K., Ouled-Cheikh, J., Prasad, S.P., Oliveros-Ramos, R., Reum, J.C., Rynne, N., Scherrer, K., Shin, Y.-J., Steenbeek, J.G., Woodworth-Jefcoats, P., Wu, Y.-L., Tittensor, D., 2024. Detecting, attributing, and projecting global marine ecosystem and Fisheries change: FishMIP 2.0. ESS Open Arch. http://dx.doi.org/10.22541/essoar.170594183.33534487/v1.

Block, B., Stevens, D., 2001. Tuna Physiology, Ecology, and Evolution. Barbara Block and E. Stevens.

Bollens, S.M., Rollwagen-Bollens, G., Quenette, J.A., Bochdansky, A.B., 2011. Cascading migrations and implications for vertical fluxes in pelagic ecosystems. J. Plankton Res. 33 (3), 349–355. http://dx.doi.org/10.1093/plankt/fbq152.

Bopp, L., Resplandy, L., Orr, J.C., Doney, S.C., Dunne, J.P., Gehlen, M., Halloran, P., Heinze, C., Ilyina, T., Séférian, R., Tjiputra, J., Vichi, M., 2013. Multiple stressors of ocean ecosystems in the 21st century: Projections with CMIP5 models. Biogeosciences 10 (10), 6225–6245. http://dx.doi.org/10.5194/bg-10-6225-2013.

Brill, R.W., 1998. How water temperature really limits the vertical movements of tunas and billfishes - Its the heart stupid. Int. Congr. Biology Fish 4.

Brill, R.W., Bigelow, K.A., Musyl, M.K., Fritsches, K.A., Warrant, E.J., 2005. Bigeye Tuna (Thunnis Obesus) Behavior and Physiology and Their Relevance to Stock Assessments and Fishery Biology. Technical Report, ICCAT.

Bruno, L., Tréguier, A.-M., Madec, G., Garnier, V., 2007. Free Surface and Variable Volume in the NEMO Code. Technical Report, Marine EnviRonment and Security for the European Area.

Buba, Y., Van Rijn, I., Blowes, S.A., Sonin, O., Edelist, D., DeLong, J.P., Belmaker, J., 2017. Remarkable size-spectra stability in a marine system undergoing massive invasion. Biology Lett. 13 (7), 20170159. http://dx.doi.org/10.1098/rsbl.2017.0159.

Burd, A.B., Hansell, D.A., Steinberg, D.K., Anderson, T.R., Arístegui, J., Baltar, F., Beaupré, S.R., Buesseler, K.O., DeHairs, F., Jackson, G.A., Kadko, D.C., Koppelmann, R., Lampitt, R.S., Nagata, T., Reinthaler, T., Robinson, C., Robison, B.H., Tamburini, C., Tanaka, T., 2010. Assessing the apparent imbalance between geochemical and biochemical indicators of meso- and bathypelagic biological activity: What the @$#! is wrong with present calculations of carbon budgets? Ecological and Biogeochemical Interactions in the Dark Ocean, Deep. Sea Res. Part II: Top. Stud. Ocean. Ecological and Biogeochemical Interactions in the Dark Ocean, 57 (16), 1557–1571.http://dx.doi.org/10.1016/j.dsr2.2010.02.022,

Butler, M., Bollens, S.M., Burkhalter, B., Madin, L.P., Horgan, E., 2001. Mesopelagic fishes of the Arabian Sea: Distribution, abundance and diet of Chauliodus pammelas, Chauliodus sloani, Stomias affinis, and Stomias nebulosus. Deep. Sea Res. Part II: Top. Stud. Ocean. 48 (6–7), 1369–1383. http://dx.doi.org/10.1016/S0967-0645(00)00143-0.

Cabello, A., Marcano, J., Narváez, M., Silva, O., Gómez, A., Figuera, B., Vallenilla, O., Salazar, H., 2003. Management of tuna resources in venezuela. Zootec. Trop. 21 (3), 261–274.

Caiger, P.E., Lefebve, L.S., Llopiz, J.K., 2021. Growth and reproduction in mesopelagic fishes: A literature synthesis. In: Proud, R. (Ed.), ICES J. Mar. Sci. 78 (3), 765–781. http://dx.doi.org/10.1093/icesjms/fsaa247.

Carvalho, P.S.M., Noltie, D.B., Tillitt, D.E., 2002. Ontogenetic improvement of visual function in the medaka *Oryzias Latipes* based on an optomotor testing system for larval and adult fish. Anim. Behav. 64 (1), 1–10. http://dx.doi.org/10.1006/anbe.2002.3028.

Chapman, R.P., Bluy, O.Z., Adlington, R.H., Robison, A.E., 1974. Deep scattering layer spectra in the Atlantic and Pacific Oceans and adjacent seas. J. Acoust. Soc. Am. 56 (6), 1722–1734. http://dx.doi.org/10.1121/1.1903504.

Checkley, D.M., Asch, R.G., Rykaczewski, R.R., 2017. Climate, anchovy, and sardine. Annu. Rev. Mar. Sci. 9 (1), 469–493. http://dx.doi.org/10.1146/annurev-marine-122414-033819.

Choy, C., Portner, E., Iwane, M., Drazen, J., 2013. Diets of five important predatory mesopelagic fishes of the central North Pacific. Mar. Ecol. Prog. Ser. 492, 169–184. http://dx.doi.org/10.3354/meps10518.

Collette, B.B., 2010. Reproduction and development in epipelagic fishes. In: Cole, K.S. (Ed.), Reproduction and Sexuality in Marine Fishes, first ed. In: Patterns and Processes, University of California Press, pp. 21–64, arXiv:10.1525/j.ctt1pp50c.6.

Craddock, J.E., Mead, G.W., 1970. Midwater fishes from the eastern South Pacific Ocean. Anton Bruun Rep.

Cury, P., Bakun, A., Crawford, R.J.M., Jarre, A., Quiñones, R.A., Shannon, L.J., Verheye, H.M., 2000. Small pelagics in upwelling systems: Patterns of interaction and structural changes in "wasp-waist" ecosystems. ICES J. Mar. Sci. 57 (3), 603–618. http://dx.doi.org/10.1006/jmsc.2000.0712.

Cury, P., Roy, C., 1989. Optimal environmental window and pelagic fish recruitment success in upwelling areas. Can. J. Fish. Aquat. Sci. 46 (4), 670–680. http://dx.doi.org/10.1139/f89-086.

da Silva, G.B., Hazin, H.G., Hazin, F.H.V., Vaske-Jr, T., 2019. Diet composition of bigeye tuna (Thunnus obesus) and yellowfin tuna (Thunnus albacares) caught on aggregated schools in the western equatorial Atlantic Ocean. J. Appl. Ichthyol. 35 (5), 1111–1118. http://dx.doi.org/10.1111/jai.13949.

Dişa, D., Akoglu, E., Salihoglu, B., 2024. Exploitation of mesopelagic fish stocks can impair the biological pump and food web dynamics in the ocean. Front. Mar. Sci. 11, http://dx.doi.org/10.3389/fmars.2024.1389941.

Dornan, T., Fielding, S., Saunders, R.A., Genner, M.J., 2019. Swimbladder morphology masks Southern Ocean mesopelagic fish biomass. Proc. R. Soc. B: Biological Sci. 286 (1903), 20190353. http://dx.doi.org/10.1098/rspb.2019.0353.

Drazen, J.C., Sutton, T.T., 2017. Dining in the deep: The feeding ecology of deep-sea fishes. Annu. Rev. Mar. Sci. 9, 337–366. http://dx.doi.org/10.1146/annurev-marine-010816-060543.

Duarte, C.M., 2015. Seafaring in the 21St century: The Malaspina 2010 circumnavigation expedition. Limnol. Ocean. Bull. 24 (1), 11–14. http://dx.doi.org/10.1002/lob.10008.

Dupont, L., Le Mézo, P., Aumont, O., Bopp, L., Clerc, C., Ethé, C., Maury, O., 2022. High trophic level feedbacks on global ocean carbon uptake and marine ecosystem dynamics under climate change. Global Change Biol. 29 (6), 1545–1556. http://dx.doi.org/10.1111/gcb.16558.

Eduardo, L.N., Mincarone, M.M., Sutton, T., Bertrand, A., 2024. Deep-pelagic fishes are anything but similar: A global synthesis. Ecol. Lett. 27 (9), e14510. http://dx.doi.org/10.1111/ele.14510.

Espinoza, P., Bertrand, A., 2008. Revisiting peruvian anchovy (*Engraulis Ringens*) trophodynamics provides a new vision of the Humboldt Current system. The Northern Humboldt Current System: Ocean Dynamics, Ecosystem Processes, and Fisheries, Prog. Oceanogr. The Northern Humboldt Current System: Ocean Dynamics, Ecosystem Processes, and Fisheries, 79 (2), 215–227. http://dx.doi.org/10.1016/j.pocean.2008.10.022,

Espinoza, P., Bertrand, A., van der Lingen, C.D., Garrido, S., Rojas de Mendiola, B., 2009. Diet of sardine (*Sardinops Sagax*) in the northern Humboldt Current system and comparison with the diets of clupeoids in this and other eastern boundary upwelling systems. Eastern Boundary Upwelling Ecosystems: Integrative and Comparative Approaches, Prog. Oceanogr. Eastern Boundary Upwelling Ecosystems: Integrative and Comparative Approaches, 83 (1), 242–250. http://dx.doi.org/10.1016/j.pocean.2009.07.045,

FAO, 2021. FAO Yearbook. Fishery and Aquaculture Statistics 2019. In: FAO, FAO, http://dx.doi.org/10.4060/cb7874t.

Faugeras, B., Maury, O., 2005. An advection-diffusion-reaction size-structured fish population dynamics model combined with a statistical parameter estimation procedure: Application to the Indian Ocean skipjack tuna Fishery. Math. Biosci. Eng. 2 (4), 719–741. http://dx.doi.org/10.3934/mbe.2005.2.719.

Fernández-Corredor, E., Francotte, L., Martino, I., Fernández-Álvarez, F.Á., García-Barcelona, S., Macías, D., Coll, M., Ramírez, F., Navarro, J., Giménez, J., 2023. Assessing juvenile swordfish (*Xiphias Gladius*) diet as an indicator of marine ecosystem changes in the northwestern Mediterranean Sea. Mar. Environ. Res. 192, 106190. http://dx.doi.org/10.1016/j.marenvres.2023.106190.

Fock, H.O., Andresen, H., Bertrand, A., Bitencourt, G., Carre, C., Couret Huertas, M., Díaz Pérez, J., Dudeck, T., Dugenne, M., Duncan, S., Figueiredo, G., Frédou, T., Garcia, X., Ghebrehiwet, D.Y., González-García, C., Kiko, R., Landeira, J.M., Lira, S., Lüskow, F., Marañón, E., Melo, P., Neumann Leitao, S., Nole Eduardo, L., Stemmann, L., Schwamborn, R., 2024. Synthetic Pelagic Biomass Size Spectra of the Tropical and Subtropical Atlantic - biovolume and carbon biomass data. http://dx.doi.org/10.5281/zenodo.13627093.

Freitas, C., Villegas-Ríos, D., Moland, E., Olsen, E.M., 2021. Sea temperature effects on depth use and habitat selection in a marine fish community. J. Anim. Ecol. 90 (7), 1787–1800. http://dx.doi.org/10.1111/1365-2656.13497.

Fujioka, K., Aoki, Y., Tsuda, Y., Okamoto, K., Tsuchida, H., Sasaki, A., Kiyofuji, H., 2024. Influence of temperature on hatching success of skipjack tuna (*Katsuwonus Pelamis*): Implications for spawning availability of warm habitats. J. Fish Biol. jfb.15767. http://dx.doi.org/10.1111/jfb.15767.

Fuller, L., Griffiths, S., Olson, R., Galván-Magaña, F., Bocanegra-Castillo, N., Alatorre-Ramírez, V., 2021. Spatial and ontogenetic variation in the trophic ecology of skipjack tuna, Katsuwonus pelamis, in the eastern Pacific Ocean. Mar. Biol. 168 (5), 73. http://dx.doi.org/10.1007/s00227-021-03872-5.

Fuller, D.W., Schaefer, K.M., Hampton, J., Caillot, S., Leroy, B.M., Itano, D.G., 2015. Vertical movements, behavior, and habitat of bigeye tuna (Thunnus obesus) in the equatorial central Pacific Ocean. Fish. Res. 172, 57–70. http://dx.doi.org/10.1016/j.fishres.2015.06.024.

Galarowicz, T.L., Adams, J.A., Wahl, D.H., 2006. The influence of prey availability on ontogenetic diet shifts of a juvenile piscivore. Can. J. Fish. Aquat. Sci. 63 (8), 1722–1733. http://dx.doi.org/10.1139/f06-073.

Galbraith, E.D., Le Mézo, P., Solanes Hernandez, G., Bianchi, D., Kroodsma, D., 2019. Growth limitation of marine fish by low iron availability in the open ocean. Front. Mar. Sci. 6, http://dx.doi.org/10.3389/fmars.2019.00509.

Gjosaeter, J., 1984. Mesopelagic fish, a large potential resource in the Arabian Sea. Deep. Sea Res. Part A. Ocean. Res. Pap. 31 (6), 1019–1035. http://dx.doi.org/10.1016/0198-0149(84)90054-2.

Gloeckler, K., Choy, C.A., Hannides, C.C.S., Close, H.G., Goetze, E., Popp, B.N., Drazen, J.C., 2018. Stable isotope analysis of micronekton around Hawaii reveals suspended particles are an important nutritional source in the lower mesopelagic and upper bathypelagic zones. Limnol. Oceanogr. 63 (3), 1168–1180. http://dx.doi.org/10.1002/lno.10762.

Gordon, J.D.M., Nishida, S., Nemoto, T., 1985. The diet of mesopelagic fish from the Pacific coast of Hokkaido, Japan. J. Ocean. Soc. Jpn. 41 (2), 89–97. http://dx.doi.org/10.1007/BF02109178.

Gorgues, T., Aumont, O., Memery, L., 2019. Simulated changes in the particulate carbon export efficiency due to diel vertical migration of zooplankton in the North Atlantic. Geophys. Res. Lett. 46 (10), 5387–5395. http://dx.doi.org/10.1029/2018GL081748.

Grady, J.M., Maitner, B.S., Winter, A.S., Kaschner, K., Tittensor, D.P., Record, S., Smith, F.A., Wilson, A.M., Dell, A.I., Zarnetske, P.L., Wearing, H.J., Alfaro, B., Brown, J.H., 2019. Metabolic asymmetry and the global diversity of marine predators. Science 363 (6425), eaat4220. http://dx.doi.org/10.1126/science.aat4220.

Graham, J., Dickson, K., 2004. Tuna comparative physiology. J. Exp. Biology 207, 4015–4024. http://dx.doi.org/10.1242/jeb.01267.

Granata, A., Bergamasco, A., Zagami, G., Guglielmo, R., Bonanzinga, V., Minutoli, R., Geraci, A., Pagano, L., Swadling, K., Battaglia, P., Guglielmo, L., 2023. Daily vertical distribution and diet of. Deep. Sea Res. Part I: Ocean. Res. Pap. 199, 104113. http://dx.doi.org/10.1016/j.dsr.2023.104113.

Grimaldo, E., Grimsmo, L., Alvarez, P., Herrmann, B., Møen Tveit, G., Tiller, R., Slizyte, R., Aldanondo, N., Guldberg, T., Toldnes, B., Carvajal, A., Schei, M., Selnes, M., 2020. Investigating the potential for a commercial Fishery in the Northeast Atlantic utilizing mesopelagic species. ICES J. Mar. Sci. 77 (7–8), 2541–2556. http://dx.doi.org/10.1093/icesjms/fsaa114.

Guiet, J., Poggiale, J.-C., Maury, O., 2016. Modelling the community size-spectrum: Recent developments and new directions. Ecol. Model. 337, 4–14. http://dx.doi.org/10.1016/j.ecolmodel.2016.05.015.

Hatton, Heneghan, Bar-On, Galbraith, 2021. The global ocean size-spectrum from bacteria to whales. Sci. Adv. http://dx.doi.org/10.5281/ZENODO.5520055.

Heneghan, R.F., Galbraith, E., Blanchard, J.L., Harrison, C., Barrier, N., Bulman, C., Cheung, W., Coll, M., Eddy, T.D., Erauskin-Extramiana, M., Everett, J.D., Fernandes-Salvador, J.A., Gascuel, D., Guiet, J., Maury, O., Palacios-Abrantes, J., Petrik, C.M., Du Pontavice, H., Richardson, A.J., Steenbeek, J., Tai, T.C., Volkholz, J., Woodworth-Jefcoats, P.A., Tittensor, D.P., 2021. Disentangling diverse responses to climate change among global marine ecosystem models. Prog. Oceanogr. 198, 102659. http://dx.doi.org/10.1016/j.pocean.2021.102659.

Hernández-Santoro, C., Landaeta, M.F., Castillo Pizarro, J., 2019. Effect of ENSO on the distribution and concentration of catches and reproductive activity of anchovy Engraulis ringens in northern Chile. Fisheries Oceanography 28 (3), 241–255. http://dx.doi.org/10.1111/fog.12405.

Herring, P.J., 1977. Bioluminescence of marine organisms. Nature 267 (5614), 788–793. http://dx.doi.org/10.1038/267788a0.

Hino, H., Kitagawa, T., Matsumoto, T., Aoki, Y., Kimura, S., 2019. Changes to vertical thermoregulatory movements of juvenile bigeye tuna (*Thunnus Obesus*) in the northwestern Pacific Ocean with time of day, seasonal ocean vertical thermal structure, and body size. Fisheries Oceanography 28 (4), 359–371. http://dx.doi.org/10.1111/fog.12417.

Holland, K., Grubbs, D., Graham, B., Itano, D., Dagorn, L., 2003. The biology of FAD-associated tuna: Temporal dynamics of association and feeding ecology. In: Meeting of the Standing Committee on Tuna and Billfish. p. 6.

Humphries, N.E., Fuller, D.W., Schaefer, K.M., Sims, D.W., 2024. Highly active fish in low oxygen environments: Vertical movements and behavioural responses of bigeye and yellowfin tunas to oxygen minimum zones in the eastern Pacific Ocean. Mar. Biol. 171 (2), 55. http://dx.doi.org/10.1007/s00227-023-04366-2.

Huston, M., Wolverton, S., 2009. The global distribution of net primary production: Resolving the paradox. Ecol. Monograph. 79, 343–377. http://dx.doi.org/10.1890/08-0588.1.

IPBES, 2019. Global Assessment Report on Biodiversity and Ecosystem Services of the Intergovernmental Science-Policy Platform on Biodiversity and Ecosystem Services. Technical Report, Zenodo, http://dx.doi.org/10.5281/zenodo.6417333.

IPCC, 2023a. Climate Change 2021 – The Physical Science Basis: Working Group I Contribution to the Sixth Assessment Report of the Intergovernmental Panel on Climate Change. Cambridge University Press, Cambridge, http://dx.doi.org/10.1017/9781009157896.

IPCC, 2023b. Climate Change 2022 – Impacts, Adaptation and Vulnerability: Working Group II Contribution to the Sixth Assessment Report of the Intergovernmental Panel on Climate Change, first ed. Cambridge University Press, http://dx.doi.org/10.1017/9781009325844.

Irigoien, X., Klevjer, T., Martinez, U., Boyra, G., Røstad, A., Wittmann, A.C., Duarte, C.M., Kaartvedt, S., Brierley, A.S., Proud, R., 2021. The Simrad EK60 echosounder dataset from the Malaspina circumnavigation. Sci. Data 8 (1), 259. http://dx.doi.org/10.1038/s41597-021-01038-y.

Irigoien, X., Klevjer, T.A., Røstad, A., Martinez, U., Boyra, G., Acuña, J.L., Bode, A., Echevarria, F., Gonzalez-Gordillo, J.I., Hernandez-Leon, S., Agusti, S., Aksnes, D.L., Duarte, C.M., Kaartvedt, S., 2014. Large mesopelagic fishes biomass and trophic efficiency in the open ocean. Nat. Commun. 5 (1), 3271. http://dx.doi.org/10.1038/ncomms4271.

Izquierdo-Peña, V., Lluch-Cota, S.E., Hernandez-Rivas, M.E., Martínez-Rincón, R.O., 2019. Revisiting the Regime Problem hypothesis: 25 years later. Deep. Sea Res. Part II: Top. Stud. Ocean. 159, 4–10. http://dx.doi.org/10.1016/j.dsr2.2018.11.003.

Jennings, S., Pinnegar, J.K., Polunin, N.V.C., Boon, T.W., 2001. Weak cross-species relationships between body size and trophic level belie powerful size-based trophic structuring in fish communities. J. Anim. Ecol. 70 (6), 934–944, arXiv:2693497.

Juanes, F., 2016. A length-based approach to predator–prey relationships in marine predators. Can. J. Fish. Aquat. Sci. 73 (4), 677–684. http://dx.doi.org/10.1139/cjfas-2015-0159.

Kaplan, D.M., Chassot, E., Amandé, J.M., Dueri, S., Demarcq, H., Dagorn, L., Fonteneau, A., 2014. Spatial management of Indian Ocean tropical tuna Fisheries: Potential and perspectives. ICES J. Mar. Sci. 71 (7), 1728–1749. http://dx.doi.org/10.1093/icesjms/fst233.

Kizenga, H.J., Jebri, F., Shaghude, Y., Raitsos, D.E., Srokosz, M., Jacobs, Z.L., Nencioli, F., Shalli, M., Kyewalyanga, M.S., Popova, E., 2021. Variability of mackerel fish catch and remotely-sensed biophysical controls in the eastern Pemba Channel. Ocean & Coastal Management 207, 105593. http://dx.doi.org/10.1016/j.ocecoaman.2021.105593.

Klevjer, T.A., Irigoien, X., Røstad, A., Fraile-Nuez, E., Benítez-Barrios, V.M., Kaartvedt., S., 2016. Large scale patterns in vertical distribution and behaviour of mesopelagic scattering layers. Sci. Rep. 6 (1), 19873. http://dx.doi.org/10.1038/srep19873.

Kobayashi, S., Ota, Y., Harada, Y., Ebita, A., Moriya, M., Onoda, H., Onogi, K., Kamahori, H., Kobayashi, C., Endo, H., Miyaoka, K., Takahashi, K., 2015. The JRA-55 reanalysis: General specifications and basic characteristics. J. Meteorol. Soc. Jpn. Ser. II 93 (1), 5–48. http://dx.doi.org/10.2151/jmsj.2015-001.

Kobyliansky, S., Orlov, A., Gordeeva, N., 2010. Composition of deepsea pelagic ichthyocenes of the Southern Atlantic, from waters of the range of the Mid-Atlantic and Walvis Ridges. J Ichthyol 50, 932–949. http://dx.doi.org/10.1134/S0032945210100036.

Kooijman, B., 2010. Dynamic Energy Budget Theory for Metabolic Organisation, third ed. Cambridge University Press, Cambridge, http://dx.doi.org/10.1017/CBO9780511805400.

Kroodsma, D.A., Mayorga, J., Hochberg, T., Miller, N.A., Boerder, K., Ferretti, F., Wilson, A., Bergman, B., White, T.D., Block, B.A., Woods, P., Sullivan, B., Costello, C., Worm, B., 2018. Tracking the global footprint of Fisheries. Science 359 (6378), 904–908. http://dx.doi.org/10.1126/science.aao5646.

Kwiatkowski, L., Torres, O., Bopp, L., Aumont, O., Chamberlain, M., Christian, J.R., Dunne, J.P., Gehlen, M., Ilyina, T., John, J.G., Lenton, A., Li, H., Lovenduski, N.S., Orr, J.C., Palmieri, J., Santana-Falcón, Y., Schwinger, J., Séférian, R., Stock, C.A., Tagliabue, A., Takano, Y., Tjiputra, J., Toyama, K., Tsujino, H., Watanabe, M., Yamamoto, A., Yool, A., Ziehn, T., 2020. Twenty-first century ocean warming, acidification, deoxygenation, and upper-ocean nutrient and primary production decline from CMIP6 model projections. Biogeosciences 17 (13), 3439–3470. http://dx.doi.org/10.5194/bg-17-3439-2020.

Langbehn, T., Aksnes, D., Kaartvedt, S., Fiksen, Ø., Jørgensen, C., 2019. Light comfort zone in a mesopelagic fish emerges from adaptive behaviour along a latitudinal gradient. Mar. Ecol. Prog. Ser. 623, http://dx.doi.org/10.3354/meps13024.

Lefort, S., Aumont, O., Bopp, L., Arsouze, T., Gehlen, M., Maury, O., 2015. Spatial and body-size dependent response of marine pelagic communities to projected global climate change. Global Change Biol. 21 (1), 154–164. http://dx.doi.org/10.1111/gcb.12679.

Lengaigne, M., Pang, S., Silvy, Y., Danielli, V., Gopika, S., Sadhvi, K., Rousset, C., Ethé, C., Person, R., Madec, G., Barrier, N., Maury, O., Menkes, C., Nicol, S., Gorgues, T., Melet, A., Guihou, K., Vialard, J., Silvy, Y., Danielli, V., Gopika, S., Sadhvi, K., Rousset, C., Ethé, C., Person, R., Madec, G., Barrier, N., Maury, O., Menkes, C., Nicol, S., Gorgues, T., Melet, A., Guihou, K., Vialard, J., 2024. An ocean-only framework for correcting future CMIP oceanic projections from their present-day biases. ESS Open Arch. http://dx.doi.org/10.22541/essoar.172019498.89258365/v1.

Lett, C., van der Lingen, C., Loveday, B., Moloney, C., 2015. Biophysical models of larval dispersal in the Benguela Current ecosystem. Afr. J. Mar. Sci. 37 (4), 457–465. http://dx.doi.org/10.2989/1814232X.2015.1105295.

Lin, C.-H., Lin, J.-S., Chen, K.-S., Chen, M.-H., Chen, C.-Y., Chang, C.-W., 2020. Feeding habits of bigeye tuna (thunnus obesus) in the western Indian ocean reveal a size-related shift in its fine-scale piscivorous diet. Front. Mar. Sci. 7, 582571. http://dx.doi.org/10.3389/fmars.2020.582571.

Lotze, H.K., Tittensor, D.P., Bryndum-Buchholz, A., Eddy, T.D., Cheung, W.W.L., Galbraith, E.D., Barange, M., Barrier, N., Bianchi, D., Blanchard, J.L., Bopp, L., Büchner, M., Bulman, C.M., Carozza, D.A., Christensen, V., Coll, M., Dunne, J.P., Fulton, E.A., Jennings, S., Jones, M.C., Mackinson, S., Maury, O., Niiranen, S., Oliveros-Ramos, R., Roy, T., Fernandes, J.A., Schewe, J., Shin, Y.-J., Silva, T.A.M., Steenbeek, J., Stock, C.A., Verley, P., Volkholz, J., Walker, N.D., Worm, B., 2019. Global ensemble projections reveal trophic amplification of ocean biomass declines with climate change. Proc. Natl. Acad. Sci. 116 (26), 12907–12912. http://dx.doi.org/10.1073/pnas.1900194116.

Lteif, M., Jemaa, S., Mouawad, R., Khalaf, G., Lelli, S., Fakhri, M., 2020. Population biology of the common pandora, *Pagellus Erythrinus* (Linnaeus, 1758) along the Lebanese coast, Eastern Mediterranean. Egypt. J. Aquat. Res. 46 (1), 57–62. http://dx.doi.org/10.1016/j.ejar.2020.01.002.

Lu, H.-J., Lee, K.-T., Lin, H.-L., Liao, C.-H., 2001. Spatio-temporal distribution of yellowfin tuna Thunnus albacares and bigeye tuna Thunnus obesus in the Tropical Pacific Ocean in relation to large-scale temperature fluctuation during ENSO episodes. Fish. Sci. 67 (6), 1046–1052. http://dx.doi.org/10.1046/j.1444-2906.2001.00360.x.

Madec, G., 2015. NEMO Ocean Engine. Technical Report, Institut Pierre-Simon Laplace, Institut Pierre-Simon Laplace.

Martin, A., Boyd, P., Buesseler, K., Cetinic, I., Claustre, H., Giering, S., Henson, S., Irigoien, X., Kriest, I., Memery, L., Robinson, C., Saba, G., Sanders, R., Siegel, D., Villa-Alfageme, M., Guidi, L., 2020. The oceans' twilight zone must be studied now, before it is too late. Nature 580 (7801), 26–28. http://dx.doi.org/10.1038/d41586-020-00915-7.

Martinez, U., Boyra, G., Irigoien, X., Klevjer, T.A., Røstad, A., Kaartvedt, S., Proud, R., Brierley, A.S., 2020. Raw EK60 Echosounder Data (38 and 120 kHz) Collected during the Malaspina 2010 Spanish Circumnavigation Expedition (14th December 2010, Cádiz - 14th July 2011, Cartagena). PANGAEA, http://dx.doi.org/10.1594/PANGAEA.921760.

Maury, O., 2005. How to Model the Size-Dependent Vertical Behavior of Bigeye (Thonnus Obesus) Tuna in Its Environment ?. Technical Report, ICCAT.

Maury, O., 2010. An overview of APECOSM, a spatialized mass balanced "Apex Predators ECOSystem Model" to study physiologically structured tuna population dynamics in their ecosystem. Prog. Oceanogr. 84 (1–2), 113–117. http://dx.doi.org/10.1016/j.pocean.2009.09.013.

Maury, O., 2017. Can schooling regulate marine populations and ecosystems? Prog. Oceanogr. 156, 91–103. http://dx.doi.org/10.1016/j.pocean.2017.06.003.

Maury, O., Poggiale, J.-C., 2013. From individuals to populations to communities: A dynamic energy budget model of marine ecosystem size-spectrum including life history diversity. J. Theoret. Biol. 324, 52–71. http://dx.doi.org/10.1016/j.jtbi.2013.01.018.

Maury, O., Poggiale, J.-C., Aumont, O., 2018. Damage-related protein turnover explains inter-specific patterns of maintenance rate and suggests modifications of the DEB theory. J. Sea Res. 143, 35–47. http://dx.doi.org/10.1016/j.seares.2018.09.021.

Maury, O., Tittensor, D.P., Eddy, T.D., Allison, E.H., Bahri, T., Barrier, N., Campling, L., Cheung, W.W.L., Frieler, K., Fulton, E.A., Guillotreau, P., Heneghan, R.F., Lam, V.W.Y., Leclère, D., Lengaigne, M., Lotze-Campen, H., Novaglio, C., Ortega-Cisneros, K., Rault, J., Schewe, J., Shin, Y.-J., Sloterdijk, H., Squires, D., Sumaila, U.R., Tidd, A.N., van Ruijven, B., Blanchard, J., 2025. The ocean system pathways (OSPs): A new scenario and simulation framework to investigate the future of the world fisheries. Earth' s Futur. 13 (3), e2024EF004851. http://dx.doi.org/10.1029/2024EF004851.

McClain-Counts, J.P., Demopoulos, A.W.J., Ross, S.W., 2017. Trophic structure of mesopelagic fishes in the Gulf of Mexico revealed by gut content and stable isotope analyses. Mar. Ecol. 38 (4), e12449. http://dx.doi.org/10.1111/maec.12449.

Mittelbach, G.G., Persson, L., 1998. The ontogeny of piscivory and its ecological consequences. Can. J. Fish. Aquat. Sci. 55 (6), 1454–1465. http://dx.doi.org/10.1139/f98-041.

Miyake, m., Guillotreau, P., Sun, C.-H., Ishimura, G., 2010. Recent developments in tuna industry: Stocks, fisheries, management, processing, trade and markets. FAO Fisheries and Aquaculture Technical Paper, FAO.

Mora, C., Tittensor, D.P., Adl, S., Simpson, A.G.B., Worm, B., 2011. How many species are there on earth and in the ocean? PLoS Biol. 9 (8), e1001127. http://dx.doi.org/10.1371/journal.pbio.1001127.

Morote, E., Olivar, M.P., Villate, F., Uriarte, I., 2010. A comparison of anchovy (Engraulis encrasicolus) and sardine (Sardina pilchardus) larvae feeding in the Northwest Mediterranean: Influence of prey availability and ontogeny. ICES J. Mar. Sci. 67 (5), 897–908. http://dx.doi.org/10.1093/icesjms/fsp302.

Muhling, B., Lamkin, J., Alemany, F., García, A., Farley, J., Ingram, J., Alvarez-Berastegui, D., Reglero, P., Laiz-Carrión, R., 2017. Reproduction and larval biology in tunas, and the importance of restricted area spawning grounds. Rev. Fish Biology Fish. 27, http://dx.doi.org/10.1007/s11160-017-9471-4.

Mullon, C., Fréon, P., Parada, C., Van Der Lingen, C., Huggett, J., 2003. From particles to individuals: Modelling the early stages of anchovy (*Engraulis Capensis/Encrasicolus*) in the southern Benguela. Fisheries Oceanography 12 (4–5), 396–406. http://dx.doi.org/10.1046/j.1365-2419.2003.00240.x.

Murphy, E.J., Cavanagh, R.D., Drinkwater, K.F., Grant, S.M., Heymans, J.J., Hofmann, E.E., Hunt, G.L., Johnston, N.M., 2016. Understanding the structure and functioning of polar pelagic ecosystems to predict the impacts of change. Proc. R. Soc. B: Biol. Sci. 283 (1844), 20161646. http://dx.doi.org/10.1098/rspb.2016.1646.

Nikolic, N., Morandeau, G., Hoarau, L., West, W., Arrizabalaga, H., Hoyle, S., Nicol, S.J., Bourjea, J., Puech, A., Farley, J.H., Williams, A.J., Fonteneau, A., 2017. Review of albacore tuna, Thunnus alalunga, biology, Fisheries and management. Rev. Fish Biology Fish. 27 (4), 775–810. http://dx.doi.org/10.1007/s11160-016-9453-y.

Novaglio, C., Bryndum-Buchholz, A., Tittensor, D., Eddy, T., Lotze, H.K., Harrison, C.S., Heneghan, R., Maury, O., Ortega-Cisneros, K., Petrik, C.M., Roberts, K.E., Blanchard, J.L., 2024. The past and future of the fisheries and marine ecosystem model intercomparison project. ESS Open Arch.

Nunn, A., Tewson, L., Cowx, I., 2012. The foraging ecology of larval and juvenile fishes. Rev. Fish Biol. Fish. 22, http://dx.doi.org/10.1007/s11160-011-9240-8.

Ohshimo, S., Hiraoka, Y., Sato, T., Nakatsuka, S., 2018. Feeding habits of bigeye tuna (Thunnus obesus) in the North Pacific from 2011 to 2013. Mar. Freshwater Res. 69 (4), 585–606. http://dx.doi.org/10.1071/MF17058.

Olsen, R.E., Strand, E., Melle, W., Nørstebø, J.T., Lall, S.P., Ringø, E., Tocher, D.R., Sprague, M., 2020. Can mesopelagic mixed layers be used as feed sources for salmon aquaculture? Structure and Functioning of the Norwegian, Iceland, Irminger and Labrador Seas Ecosystems: A Comparative Study, Deep. Sea Res. Part II: Top. Stud. Ocean. Structure and Functioning of the Norwegian, Iceland, Irminger and Labrador Seas Ecosystems: A Comparative Study, 180, 104722.http://dx.doi.org/10.1016/j.dsr2.2019.104722,

Patterson, T.A., Eveson, J.P., Hartog, J.R., Evans, K., Cooper, S., Lansdell, M., Hobday, A.J., Davies, C.R., 2018. Migration dynamics of juvenile southern bluefin tuna. Sci. Rep. 8 (1), 14553. http://dx.doi.org/10.1038/s41598-018-32949-3.

Pearcy, W.G., Lorz, H.V., Peterson, W., 1979. Comparison of the feeding habits of migratory and non-migratory Stenobrachius leucopsarus (Myctophidae). Mar. Biol. 51 (1), 1–8. http://dx.doi.org/10.1007/BF00389025.

Pérez, V., Fernández, E., Marañón, E., Morán, X.A.G., Zubkov, M.V., 2006. Vertical distribution of phytoplankton biomass, production and growth in the Atlantic subtropical gyres. Deep. Sea Res. Part I: Ocean. Res. Pap. 53 (10), 1616–1634. http://dx.doi.org/10.1016/j.dsr.2006.07.008.

Plank, M.J., 2011. Effects of predator diet breadth on stability of size spectra. ANZIAM J. 53 (1), 38–47. http://dx.doi.org/10.1017/S1446181112000041.

Potier, M., Marsac, F., Lucas, V., Sabatié, R., Hallier, J.-P., Ménard, F., 2004. Feeding partitioning among tuna taken in surface and mid-water layers: The case of yellowfin (thunnus albacares) and bigeye (T. Obesus) in the western tropical Indian ocean. West. Indian Ocean. J. Mar. Sci. 3 (1), 51–62.

Priede, I., 2017. Deep-Sea Fishes: Biology, Diversity, Ecology and Fisheries. Cambridge University Press, http://dx.doi.org/10.1017/9781316018330.

Proud, R., Handegard, N.O., Kloser, R.J., Cox, M.J., Brierley, A.S., 2019. From siphonophores to deep scattering layers: Uncertainty ranges for the estimation of global mesopelagic fish biomass. In: Demer, D. (Ed.), ICES J. Mar. Sci. 76 (3), 718–733. http://dx.doi.org/10.1093/icesjms/fsy037.

Puvanendran, V., Brown, J.A., 2002. Foraging, growth and survival of Atlantic cod larvae reared in different light intensities and photoperiods. Aquaculture 214 (1), 131–151. http://dx.doi.org/10.1016/S0044-8486(02)00045-5.

Ragoasha, N., Herbette, S., Cambon, G., Veitch, J., Reason, C., Roy, C., 2019. Lagrangian pathways in the southern Benguela upwelling system. J. Mar. Syst. 195, 50–66. http://dx.doi.org/10.1016/j.jmarsys.2019.03.008.

Riaz, J., Walters, A., Trebilco, R., Bestley, S., Lea, M.-A., 2020. Stomach content analysis of mesopelagic fish from the southern Kerguelen Axis. Ecosystem Drivers of Food Webs on the Kerguelen Axis of the Southern Ocean, Deep. Sea Res. Part II: Top. Stud. Ocean. Ecosystem Drivers of Food Webs on the Kerguelen Axis of the Southern Ocean, 174, 104659.http://dx.doi.org/10.1016/j.dsr2.2019.104659,

Robinson, C.J., Anislado, V., Lopez, A., 2004. The pelagic red crab (Pleuroncodes planipes) related to active upwelling sites in the California Current off the West Coast of Baja California. Deep. Sea Res. Part II: Top. Stud. Ocean. 51 (6–9), 753–766. http://dx.doi.org/10.1016/j.dsr2.2004.05.018.

Robinson, C., Steinberg, D.K., Anderson, T.R., Arístegui, J., Carlson, C.A., Frost, J.R., Ghiglione, J.-F., Hernández-León, S., Jackson, G.A., Koppelmann, R., Quéguiner, B., Ragueneau, O., Rassoulzadegan, F., Robison, B.H., Tamburini, C., Tanaka, T., Wishner, K.F., Zhang, J., 2010. Mesopelagic zone ecology and biogeochemistry – a synthesis. Ecological and Biogeochemical Interactions in the Dark Ocean, Deep. Sea Res. Part II: Top. Stud. Ocean. Ecological and Biogeochemical Interactions in the Dark Ocean, 57 (16), 1504–1518. http://dx.doi.org/10.1016/j.dsr2.2010.02.018,

Rodhouse, P.G., White, M.G., 1995. Cephalopods occupy the ecological niche of epipelagic fish in the antarctic polar frontal zone. Biological Bull. 189 (2), 77–80. http://dx.doi.org/10.2307/1542457.

Romero, J., Catry, P., Hermida, M., Neves, V., Cavaleiro, B., Gouveia, L., Granadeiro, J.P., 2021. Tunas off northwest Africa: The epipelagic diet of the bigeye and skipjack tunas. Fish. Res. 238, 105914. http://dx.doi.org/10.1016/j.fishres.2021.105914,

Rose, K., Morrone, J., Doney, S., Coles, V., Reygondeau, G., Cheung, W., Wabnitz, C., Lam, V., Frölicher, T., Maury, O., 2020. Climate change-induced emergence of novel biogeochemical provinces. Front. Mar. Sci. 7, 657. http://dx.doi.org/10.3389/fmars.2020.00657.

Røstad, A., Kaartvedt, S., Aksnes, D.L., 2016. Light comfort zones of mesopelagic acoustic scattering layers in two contrasting optical environments. Deep. Sea Res. Part I: Ocean. Res. Pap. 113, 1–6. http://dx.doi.org/10.1016/j.dsr.2016.02.020.

Sanders, R.J., Henson, S.A., Martin, A.P., Anderson, T.R., Bernardello, R., Enderlein, P., Fielding, S., Giering, S.L.C., Hartmann, M., Iversen, M., Khatiwala, S., Lam, P., Lampitt, R., Mayor, D.J., Moore, M.C., Murphy, E., Painter, S.C., Poulton, A.J., Saw, K., Stowasser, G., Tarling, G.A., Torres-Valdes, S., Trimmer, M., Wolff, G.A., Yool, A., Zubkov, M., 2016. Controls over Ocean mesopelagic interior carbon storage (COMICS): Fieldwork, synthesis, and modeling efforts. Front. Mar. Sci. 3, http://dx.doi.org/10.3389/fmars.2016.00136.

Scharf, F.S., Juanes, F., Rountree, R.A., 2000. Predator size-prey size relationships of marine fish predators: Interspecific variation and effects of ontogeny and body size on trophic-niche breadth. Mar. Ecol. Prog. Ser. 208, 229–248. http://dx.doi.org/10.3354/meps208229.

Sheldon, R.W., Prakash, A., Sutcliffe, W.H., 1972. The size distribution of particles in the ocean. Limnol. Oceanogr. 17 (3), 327–340. http://dx.doi.org/10.4319/lo.1972.17.3.0327.

Smith, C.R., Berelson, W., Demaster, D.J., Dobbs, F.C., Hammond, D., Hoover, D.J., Pope, R.H., Stephens, M., 1997. Latitudinal variations in benthic processes in the abyssal equatorial Pacific: Control by biogenic particle flux. A JGFOS Process Study in the Equatorial Pacific, Deep. Sea Res. Part II: Top. Stud. Ocean. A JGFOS Process Study in the Equatorial Pacific, 44 (9), 2295–2317. http://dx.doi.org/10.1016/S0967-0645(97)00022-2,

Smith, C.R., Demopoulos, A.W.J., 2003. The deep Pacific ocean floor. Ecosyst. World.

Smith, C.R., Leo, F.C.D., Bernardino, A.F., Sweetman, A.K., Arbizu, P.M., 2008. Abyssal food limitation, ecosystem structure and climate change. Trends Ecol. Evolut. 23 (9), 518–528. http://dx.doi.org/10.1016/j.tree.2008.05.002.

Sprules, W., Kerr, S., Dickie, L., 2002. The biomass spectrum: A predator-prey theory of aquatic production. Ecology 83, http://dx.doi.org/10.2307/3071789.

St. John, M.A., Borja, A., Chust, G., Heath, M., Grigorov, I., Mariani, P., Martin, A.P., Santos, R.S., 2016. A dark hole in our understanding of marine ecosystems and their services: Perspectives from the mesopelagic community. Front. Mar. Sci. 3, http://dx.doi.org/10.3389/fmars.2016.00031.

Sutton, T.T., 2013. Vertical ecology of the pelagic ocean: Classical patterns and new perspectives. J. Fish Biol. 83 (6), 1508–1527. http://dx.doi.org/10.1111/jfb.12263.

Sutton, T.T., Clark, M.R., Dunn, D.C., Halpin, P.N., Rogers, A.D., Guinotte, J., Bograd, S.J., Angel, M.V., Perez, J.A.A., Wishner, K., Haedrich, R.L., Lindsay, D.J., Drazen, J.C., Vereshchaka, A., Piatkowski, U., Morato, T., Błachowiak-Samołyk, K., Robison, B.H., Gjerde, K.M., Pierrot-Bults, A., Bernal, P., Reygondeau, G., Heino, M., 2017. A global biogeographic classification of the mesopelagic zone. Deep. Sea Res. Part I: Ocean. Res. Pap. 126, 85–102. http://dx.doi.org/10.1016/j.dsr.2017.05.006.

Taconet, P., Chassot, E., Barde, J., 2018. Global Monthly Catch of Tuna, Tuna-like and Shark Species (1950–2015) Aggregated by 1° or 5° Squares (IRD Level 2). Zenodo, http://dx.doi.org/10.5281/zenodo.1164128.

Taconet, M., Kroodsma, D., Fernandes, J., 2019. Global Atlas of AIS-based Fishing Activity. Technical Report, FAO.

Tagliabue, A., Twining, B.S., Barrier, N., Maury, O., Berger, M., Bopp, L., 2023. Ocean iron fertilization may amplify climate change pressures on marine animal biomass for limited climate benefit. Global Change Biol. 29 (18), 5250–5260. http://dx.doi.org/10.1111/gcb.16854.

Takyi, R., Addo, C., El Mahrad, B., Adade, R., ElHadary, M., Nunoo, F.K.E., Essandoh, J., Chuku, E.O., Iriarte-Ahon, F., 2023. Marine Fisheries management in the Eastern Central Atlantic Ocean. Ocean & Coastal Management 244, 106784. http://dx.doi.org/10.1016/j.ocecoaman.2023.106784.

Thompson, S.E., Kenchington, T.J., 2017. Distribution and diet of Cyclothone microdon (Gonostomatidae) in a submarine canyon. J. Mar. Biol. Assoc. UK 97 (8), 1573–1580. http://dx.doi.org/10.1017/S0025315416000916.

Thums, M., Meekan, M., Stevens, J., Wilson, S., Polovina, J., 2013. Evidence for behavioural thermoregulation by the world's largest fish. J. R. Soc. Interface 10 (78), 20120477. http://dx.doi.org/10.1098/rsif.2012.0477.

Tittensor, D.P., Eddy, T.D., Lotze, H.K., Galbraith, E.D., Cheung, W., Blanchard, J.L., Bopp, L., Bryndum-Buchholz, A., Büchner, M., Bulman, C., Carozza, D.A., Christensen, V., Coll, M., Dunne, J.P., Fulton, E.A., Hobday, A.J., Huber, V., Jennings, S., Jones, M., Lehodey, P., Link, J.S., Mackinson, S., Maury, O., Oliveros-Ramos, R., Roy, T., Schewe, J., Shin, Y.-J., Stock, C.A., Steenbeek, J., Underwood, P.J., Volkholz, J., Walker, N.D., 2018. A protocol for the intercomparison of marine Fishery and ecosystem models: Fish-MIP v1.0. Geosci. Model. Dev.

Tittensor, D.P., Novaglio, C., Harrison, C.S., Heneghan, R.F., Barrier, N., Bianchi, D., Bopp, L., Bryndum-Buchholz, A., Britten, G.L., Büchner, M., Cheung, W.W.L., Christensen, V., Coll, M., Dunne, J.P., Eddy, T.D., Everett, J.D., Fernandes-Salvador, J.A., Fulton, E.A., Galbraith, E.D., Gascuel, D., Guiet, J., John, J.G., Link, J.S., Lotze, H.K., Maury, O., Ortega-Cisneros, K., Palacios-Abrantes, J., Petrik, C.M., Du Pontavice, H., Rault, J., Richardson, A.J., Shannon, L., Shin, Y.-J., Steenbeek, J., Stock, C.A., Blanchard, J.L., 2021. Next-generation ensemble projections reveal higher climate risks for marine ecosystems. Nat. Clim. Chang. 11 (11), 973–981. http://dx.doi.org/10.1038/s41558-021-01173-9.

Tsukamoto, K., Miller, M.J., 2021. The mysterious feeding ecology of leptocephali: A unique strategy of consuming marine snow materials. Fish. Sci. 87 (1), 11–29. http://dx.doi.org/10.1007/s12562-020-01477-3.

Valls Mir, M., Olivar, M., Fernández de Puelles, M., Molí, B., Bernal Bajo, A., Sweeting, C., 2014. Trophic structure of mesopelagic fishes in the western Mediterranean based on stable isotopes of carbon and nitrogen. J. Mar. Syst. 138, 160–170. http://dx.doi.org/10.1016/j.jmarsys.2014.09.001.

Van Der Lingen, C.D., 2002. Diet of sardine Sardinops sagax in the southern Benguela upwelling ecosystem. S. Afr. J. Mar. Sci. 24 (1), 301–316. http://dx.doi.org/10.2989/025776102784528691.

van der Lingen, C., Bertrand, A., Bode, A., Brodeur, R., Cubillos, L., Espinoza, P., Friedland, K., Garrido, S., Irigoien, X., Miller, T., Möllmann, C., Rodriguez-Sanchez, R., Tanaka, H., Temming, A., 2009. Trophic dynamics of small pelagic fish. In: Synthesis Book of the Program "Small Pelagic Fish and Climate Change Program (SPACC)". Cambridge University Press, pp. 333–403.

Varela, J.L., Abascal, F.J., Medina, A., 2023. Foraging patterns and trophic interactions of sympatric populations of Young-of-the-year bluefin and skipjack tunas in the East Atlantic (Gulf of Cadiz). Reg. Stud. Mar. Sci. 62, 102961. http://dx.doi.org/10.1016/j.rsma.2023.102961.

Watch, G.F., 2023. Jumbo Squid Fishery | Southeast Pacific Ocean.

Watson, J.R., Stock, C.A., Sarmiento, J.L., 2015. Exploring the role of movement in determining the global distribution of marine biomass using a coupled hydrodynamic – Size-based ecosystem model. Combining Modeling and Observations to Better Understand Marine Ecosystem Dynamics, Prog. Oceanogr. Combining Modeling and Observations to Better Understand Marine Ecosystem Dynamics, 138, 521–532.http://dx.doi.org/10.1016/j.pocean.2014.09.001,

Yapur-Pancorvo, A.L., Quispe-Machaca, M., Guzmán-Rivás, F., Urzúa, Á., Espinoza, P., 2023. The red squat lobster pleuroncodes monodon in the humboldt current system: From their ecology to commercial attributes as marine bioresource. Animals 13 (14), 2279. http://dx.doi.org/10.3390/ani13142279.

Young, R.E., 1983. Oceanic bioluminescence: An overview of general functions. Bull. Mar. Sci. 33 (4), 829–845.

Zhang, L., Thygesen, U.H., Knudsen, K., Andersen, K.H., 2013. Trait diversity promotes stability of community dynamics. Theor. Ecol. 6 (1), 57–69. http://dx.doi.org/10.1007/s12080-012-0160-6.

Zhou, M., 2006. What determines the slope of a plankton biomass spectrum? J. Plankton Res. 28 (5), 437–448. http://dx.doi.org/10.1093/plankt/fbi119.

Zhou, C., Wan, R., Cao, J., Xu, L., Wang, X., Zhu, J., 2021. Spatial variability of bigeye tuna habitat in the Pacific Ocean: Hindcast from a refined ecological niche model. Fisheries Oceanography 30 (1), 23–37. http://dx.doi.org/10.1111/fog.12500.